Journal of Medicinal Chemistry

Article

pubs.acs.org/jmc

Identification of NVP-TNKS656: The Use of Structure–Efficiency Relationships To Generate a Highly Potent, Selective, and Orally Active Tankyrase Inhibitor

Michael D. Shultz,* Atwood K. Cheung, Christina A. Kirby, Brant Firestone, Jianmei Fan, Christine Hiu-Tung Chen, Zhouliang Chen, Donovan N. Chin, Lucian DiPietro,‡ Aleem Fazal, Yun Feng, Pascal D. Fortin, Ty Gould, Bharat Lagu, Huangshu Lei,§ Francois Lenoir, Dyuti Majumdar, Etienne Ochala,∥ M. G. Palermo, Ly Pham,⊥ Minying Pu, Troy Smith, Travis Stams, Ronald C. Tomlinson,# B. Barry Touré, Michael Visser, Run Ming Wang, Nigel J. Waters,□ and Wenlin Shao

Novartis Institutes for Biomedical Research, Inc., 250 Massachusetts Avenue, Cambridge, Massachusetts 02139, United States

Supporting Information

ABSTRACT: Tankyrase 1 and 2 have been shown to be redundant, druggable nodes in the Wnt pathway. As such, there has been intense interest in developing agents suitable for modulating the Wnt pathway in vivo by targeting this enzyme pair. By utilizing a combination of structure-based design and LipE-based structure efficiency relationships, the core of XAV939 was optimized into a more stable, more efficient, but less potent dihydropyran motif **7**. This core was combined with elements of screening hits **2**, **19**, and **33** and resulted in highly potent, selective tankyrase inhibitors that are novel three pocket binders. NVP-TNKS656 (**43**) was identified as an orally active antagonist of Wnt pathway activity in the MMTV-Wnt1 mouse xenograft model. With an enthalpy-driven thermodynamic signature of binding, highly favorable physicochemical properties, and high lipophilic efficiency, NVP-TNKS656 is a novel tankyrase inhibitor that is well suited for further in vivo validation studies.

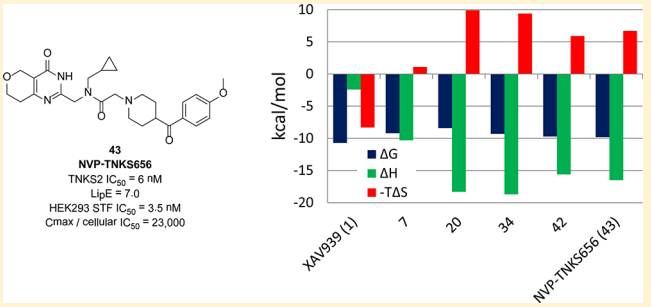

INTRODUCTION

Tankyrase (TNKS) proteins are multifunctional poly(ADP-ribose) polymerases (PARPs), which are enzymes utilizing NAD^+ as a substrate to generate ADP-ribose polymers onto target proteins (PARsylation).[1] Both isoforms of TNKS, TNKS1 and TNKS2, share overlapping functions and similar structures, including the ankyrin (ANK) repeat domain, the SAM domain (sterile alpha molecule), and the catalytic PARP domain.[2] The ankyrin domain is important for mediating protein–protein interactions, and the SAM domain mediates mono- and heteromultimerization of TNKS. Through binding and modulating substrate proteins, TNKS plays a role in regulating a variety of cellular processes, including telomere regulation, mitotic spindle pole function, membrane translocation of Golgi-associated vesicles upon insulin stimulation, and B cell antigen receptor activation.[2−4] Previous findings from our group have shown that TNKS could regulate the activity of the Wnt/β-catenin pathway in colon cancer cells through PARsylation and destabilization of the axin proteins.[5] In addition to the aforementioned substrates, an array of proteins representing diverse biological functions have been predicted to be TNKS targets on the basis of structural and sequence information of TNKS targeting proteins.[6] The broad biological role of TNKS thus offers an opportunity for its therapeutic intervention in diseases where TNKS substrates become dysregulated, such as telomere elongation in cancer, Wnt pathway activation in cancer, and cardiovascular and neurodegenerative diseases.[7] Indeed, multiple groups have reported identification of TNKS inhibitors from high throughput screens and chemical optimization (Figure 1).[4,8−10] These inhibitors have been investigated for their utilities in the treatment of cancer, fibrosis, herpes simplex virus replication, and remyelination, providing important insight on therapeutic indications of targeting TNKS.[4,10−15]

We recently described the characterization of a novel series of selective dual inhibitors of TNKS1/2 (**2**) that are devoid of activity against PARP1 or PARP2 (Figure 1).[9] These inhibitors exhibit low nanomolar TNKS inhibition and submicromolar activity in inhibiting Wnt pathway signaling. Others have recently published optimization efforts that have resulted in G007-LK and compound **44**.[16−18] In this report, we explore a novel use of lipophilic efficiency (LipE = $pIC_{50} - \log P$)[19] to survey a diverse range of chemical structures to more effectively

Received: May 30, 2013

   dx.doi.org/10.1021/jm400807n | J. Med. Chem. XXXX, XXX, XXX–XXX

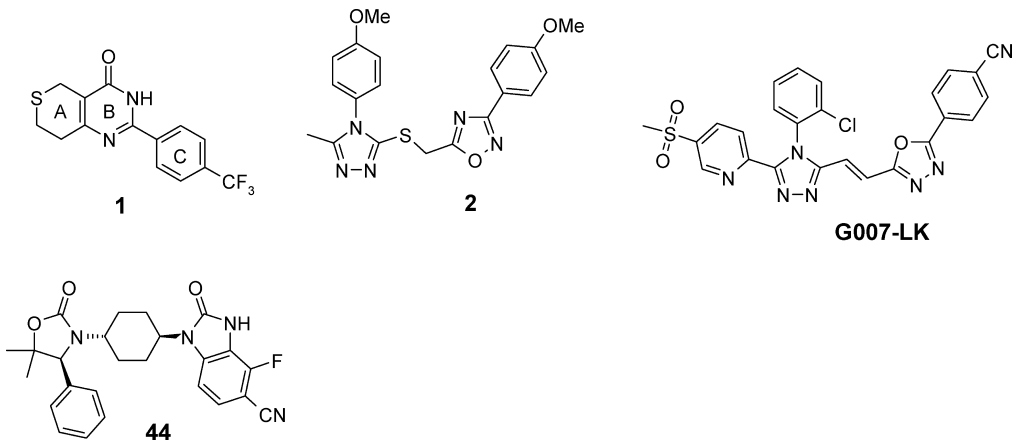

Figure 1. Select TNKS inhibitors that have been reported in the literature.

Table 1. A-Ring Modifications of 1

Compound	Structure	TNKS2 LipE[a]	IC$_{50}$ (μM) TNKS2	TNKS1	PARP1	PARP2	STF[b]	clogP	RLM ER[c]
1	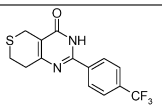	5.9 4.2[e]	0.0053	0.013	1.37	0.106	0.078	2.3 4.1[d]	0.88
3	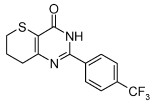	2.8	0.032	0.110	10.5	4.08	1.72	3.1	0.97
4	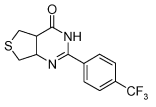	5.0	0.127	0.262	>19	-	5.04	1.9	0.96
5	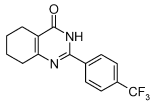	3.5	0.163	0.093	11.2	-	1.41	3.3	0.80
6	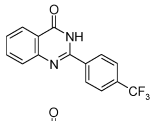	4.4	0.0215	0.050	-	-	1.67	3.3	0.56
7	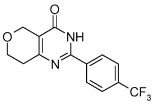	5.9 4.0[e]	0.075	-	>19	-	2.65	1.2 3.1[d]	0.24
8	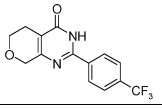	5.2	0.378	0.485			18.1	1.2	0.49

[a]LipE = pIC$_{50}$ (TNKS2) − clogP. [b]HEK293 SuperTopFlash reporter gene assay. [c]Rat liver microsome extraction ratio. [d]Measured log *D*. [e]LipE = pIC$_{50}$ (TNKS2) − log *D*.

understand what are the most efficient interactions favored by TNKS. With this information, we were able to develop TNKS inhibitors with improved activity, selectivity, and pharmacokinetic profiles for in vivo testing.

Following our identification of XAV939 (**1**), our initial hit finding efforts discovered several series of TNKS inhibitors that were evaluated and prioritized for further optimization.[5,9] In parallel, we evaluated **1** to identify potential liabilities and devise an optimization strategy. There are several attributes of **1** which make it an attractive starting point including low nanomolar biochemical activity, 78 nM cellular activity, high ligand efficiency[20] (LE = 0.55), and good lipophilic efficiency (LipE = 4.2 based on measured log *D* of 4.1). Unfortunately, **1** is not without liabilities which include low selectivity versus other PARP family members (10−100 fold), low microsomal stability (rat liver microsomal extraction ration, rLMER = 0.88), and low solubility (10 μM at pH1, < 5 μM at pH 6.8) which hampered the use of reasonable formulations for in vivo studies. For a preclinical proof of concept on the impact of TNKS inhibition in model systems, a potent, selective, and in vivo active TNKS inhibitor was required; therefore, the highest priority for this series was to increase potency, selectivity, solubility, and metabolic stability. Because compound **1** had a measured log *D* of 4.1, it was hypothesized that by reducing the lipophilicity the off-target liabilities and poor properties could be improved.[21]

Lipophilic efficiency[19] (LipE = pIC$_{50}$ − log *D*) provides a convenient measure of the differential between potency and

dx.doi.org/10.1021/jm400807n | J. Med. Chem. XXXX, XXX, XXX−XXX

Scheme 1. Synthesis of A-Ring Analogues[a]

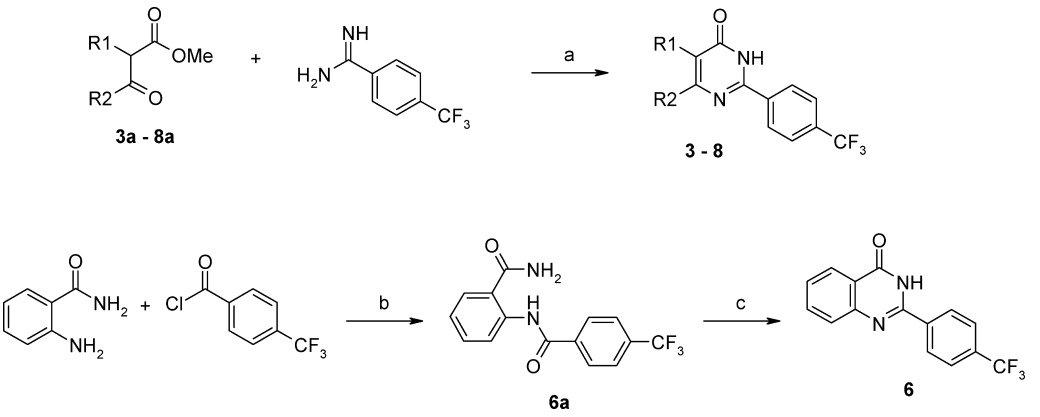

[a](a) K_2CO_3, MeOH, 75 °C; (b) DIEA, THF; (c) KOEt, 140 °C, 20 min.

lipophilicity and therefore was ideally aligned with our optimization goals. It should be noted in Table 1 that early on we identified a significant disconnect between calculated logP and measured log *P*/*D* for this series (Supporting Information Figures 1 and 2), and therefore the LipE calculations throughout this manuscript will be artificially high relative to those based on measured log *D*. There are several points that should be made at the outset to better understand how the LipE tool might best be used. First, because there can be errors in clogP calculations, comparison of highly dissimilar structural classes should be performed with caution and preferably utilizing measured log *D* values. Second, for structure−efficiency relationships (SER), it is the change in LipE (ΔLipE) between matched pairs that is meaningful in decision making. If a change between a molecular matched pair (MMP)[22] is unlikely to introduce an ionizable group or affect the pK_a of an existing one, then ΔclogP can be calculated with high accuracy and should correlate very well with changes in measured log *P* and log *D*, and therefore may be used with confidence (Supporting Information Figure 2). Finally, although it has been reported that there are target LipE values for optimization,[19,23,24] these are highly theoretical and likely target dependent. Thus, we do not support using an absolute LipE value to determine if sufficient optimization has been achieved. We were very interested in evaluating the utility of LipE for enhanced decision making based on SER and describe herein the results of using LipE for making nonobvious choices during an iterative optimization process. While we report ligand efficiency for **1**, we did not use this parameter during our optimization efforts and only SER utilizing LipE will be discussed.

For all compounds in Table 1 and throughout this manuscript (with the exception of compound **4**), potency against TNKS2 was typically 2−10 fold greater than TNKS1. No significant selectivity between these isoforms was observed for compounds in this manuscript; therefore, this data is not reported in subsequent tables.

RESULTS AND DISCUSSION

Computational programs that predict oxidative metabolism such as Metasite and Stardrop support the concern that we had at the outset of the optimization process that the A-ring sulfur was a likely soft spot for oxidative metabolism (Supporting Information Figure 3), and so replacement of this moiety was our initial goal.[23−26] Modification of the XAV939 A-ring was accomplished by the condensation of keto ester derivatives with an appropriate amidine moiety (Scheme 1). Compound **1**, a nicotinamide mimetic, is structurally similar to many previously reported PARP antagonists,[7] and we generated a series of analogues where the sulfur-containing ring was altered (Table 1). For the nonaromatic A-rings analogues (**3**−**5**), it became clear that all changes were not well tolerated as potency and LipE decreased. Aromatization of ring A (**6**) did improve the microsomal stability but was a less efficient inhibitor.

We hypothesized that an oxygen-containing A-ring, such as a dihydropyran, could improve solubility and metabolic stability; therefore, we synthesized several of these analogues (e.g., **7** and **8**). All analogues were more polar than **1** but also less potent. Compound **7** is 33-fold less potent in the cellular assay than **1**, a result that would typically remove this modification from further consideration; however, these two compounds have identical LipE values and therefore **7** was evaluated further. With a solubility improvement of at least 10-fold and an even more substantial improvement in microsomal stability, **7** was able to be formulated for a rat pharmacokinetic (PK) study via intravenous (iv) administration. After iv administration to Sprague−Dawley rats, good exposure of compound **7** with low clearance (8.9 mL/min/kg) and a high volume of distribution (Vdss = 2.7 L/kg) was observed. The PK profile 2 h postdose suggests the possibility of enterohepatic recirculation, which is plausible because of the available hydroxyl for direct conjugation and biliary elimination. However, this hypothesis would need to be further evaluated in mechanistic studies.

With the higher selectivity toward PARP 1 and 2 (50−1300 fold,) we decided to preserve the dihydropyran motif and shift optimization to the other side of the molecule. The synthesis of C-ring modifications is outlined in Scheme 2. In an attempt to identify the minimal pharmacophore required for inhibition, the phenyl ring was removed or replaced with heterocycles which led to the complete loss of activity with the exception of **9**

Scheme 2. Synthesis of Dihydropyran C-Ring Analogues[a]

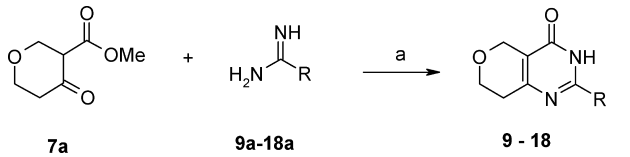

[a]K_2CO_3, MeOH, reflux overnight.

dx.doi.org/10.1021/jm400807n | J. Med. Chem. XXXX, XXX, XXX−XXX

(Table 2). The improved LipE of **9**, relative to the other analogues, suggests that the phenyl ring was suboptimal. We

Table 2. Structure−Efficiency Relationships of C-Ring Analogues

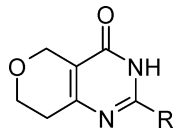

Compound	Structure	TNKS2 LipE[a]	IC$_{50}$ (μM) TNKS2	IC$_{50}$ (μM) STF[b]	clogP	RLM ER[c]
7	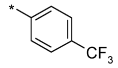	5.9	0.075	2.67	1.2	0.24
9		6.9	0.136	8.09	-0.03	-
10	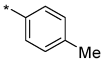	6.4	0.062	4.63	0.78	-
11	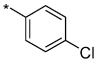	5.8	0.148	4.43	1.0	-
12	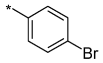	5.9	0.081	4.14	1.2	-
13	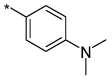	6.8	0.041	4.21	0.58	-
14	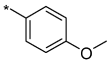	6.8	0.086	5.05	0.32	-
15	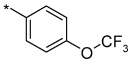	5.8	0.055	1.22	1.4	0.22
16	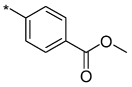	6.4	0.202	3.00	0.28	-
17	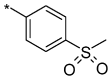	8.4	0.063	6.29	-1.2	0.18
18	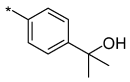	7.7 7.1[e]	0.022	1.03	-0.05 0.52[d]	0.23

[a]LipE = pIC$_{50}$ (TNKS2) − clogP. [b]HEK293 SuperTopFlash reporter gene assay. [c]Rat liver microsome extraction ratio. [d]Measured log *D*. [e]LipE = pIC$_{50}$ (TNKS2) − log *D*.

next explored a series of trifluoromethyl replacements (**10**−**17**) to probe this region. Replacement of the trifluoromethyl group with a methyl group did not affect potency but resulted in improved LipE due to a reduction in lipophilicity, perhaps an indication that more optimal groups could be identified. A broad range of analogues were tested and significant improvements in LipE with several compounds (**13**, **14**, **16**, and especially **17**) were observed. However, this diverse range of substitutions all resulted in similar activity (20−200 nM). Closer examination of the crystal structure revealed that most of the substituents in this subseries are solvent-exposed and have very little interaction with the TNKS protein. In contrast, modifications at the ortho position of the C-ring obliterates activity (data not shown). We observed that LipE values can be increased with polar groups that interact with the bulk solvent, and while this may improve a compound's overall profile, in the context of efficient binding it has little to do with direct interactions with TNKS.

The optimization appeared to have entered a structural cul-de-sac where the vectors off of the C-ring were not favorable for further optimization but did allow for modulation of the overall properties of the molecule. While most of this position was solvent-exposed, we hypothesized that an amphipathic group might allow for some hydrophobic TNKS−ligand interactions while also assisting in overall properties by lowering log *D*. Whereas compound **17** has two polar oxygens and one methyl group, we sought an analogue with a single hydrophobic and hydrophilic group. The additional methyl group of **18** improved LipE relative to **7** (7.1 based on measured log *D*) and apparently efficiency peaked at **17** and **18** as other analogues (not shown) had slightly improved potency but significantly lower LipE. Compound **18** was further evaluated and found to be extremely stable in liver microsomes (rER = 0.23), over 500-fold more soluble than **1**, and on the basis of measured log *D* values had significantly greater lipophilic efficiency (ΔLipE = +2.9). Suitable formulations for multiple dose pharmacokinetic (PK)/pharmacodynamic (PD)/efficacy studies with compound **18** were achieved, and further in vivo characterization was performed.

The pharmacokinetics of compound **18** was evaluated in both rats and mice. After oral administration in Sprague−Dawley rats, compound **18** showed good overall exposure and bioavailability (F = 46%) where an initial rapid phase of absorption was observed, followed by a second peak at 6 h postdose. After iv administration, compound **18** again displayed good exposure and low clearance (12 mL/min/kg), in line with the low in vitro clearance prediction in rat liver microsomes (ER = 0.24). Similar to the iv profile of compound **7**, the concentration versus time profile of compound **18** after oral administration also displayed a second peak 4−6 h postdose, further supporting the earlier hypothesis for enterohepatic recirculation of either parent or a direct glucuronidation of the free hydroxyl. In mice, compound **18** showed dose-proportional exposure after oral dosing and good bioavailability (F = 32%). **18** also showed moderate iv clearance in good agreement with the in vitro clearance prediction from mouse liver microsomes. While high oral doses (300 mg/kg) were tolerated, the low cellular potency only allowed for total drug concentrations to exceed the cellular IC$_{50}$ values for 4−5 h.

It was becoming increasingly clear that modifications based on the ABC rings of **1** would not be able to achieve the low nanomolar potency we required, and therefore we sought a more favorable scaffold where the C ring was completely replaced. At this time, we obtained a crystal structure of the TNKS1 PARP domain in complex with an interesting screening hit (**19**) to 2.1 Å resolution. The compound bound to the NAD$^+$ donor site, occupying the nicotinamide and diphosphate pockets. Its interactions with TNKS1 mimic those seen in the structure of TNKS1 in complex with XAV939[24] which include stacking interactions of the pyrimidine ring with Tyr1224 and hydrogen bonds between the hydroxyl of Ser1221 and Gly1185 with the pyrimidine hydroxyl and pyrimidine nitrogen, respectively. Additionally, **19** takes advantage of a previously defined hydrophobic nook[9] where the thiophene moiety makes van der Waals interactions with Cβ of Ser1186, Pro1187, and Ile1228. Additionally, the phenyl ring makes van der Waals interactions with His1184, Ser1186, and Phe1188. Unfortunately, **19** had poor solubility and low microsomal stability, consistent with the lower LipE (Table 3). By converting the A ring into the dihydropyran motif (compound **20**), the LipE (4.5 based on measured log *D*) and solubility improved dramatically,

dx.doi.org/10.1021/jm400807n | J. Med. Chem. XXXX, XXX, XXX−XXX

Table 3. Structure−Efficiency Relationships of Compounds 1, 7, and 19 Tribrid Analogues

Compound	Structure	TNKS2 LipE[a]	IC_{50} (μM) TNKS2	PARP1	PARP2	STF[b]	clogP	RLM ER[c]
1	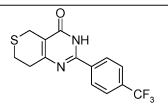	5.9	0.0053	1.37	0.106	0.078	2.3	0.88
19	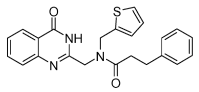	4.5 3.2[e]	0.106	18.2	-	0.937	2.5 3.8[d]	>0.97
20	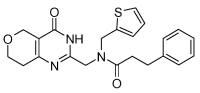	6.2 4.4[e]	0.216	-	56.4	1.92	0.42 2.2[d]	0.95
21	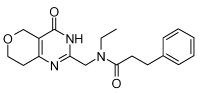	5.7	4.78	-	-	>50	-0.37	0.61
22	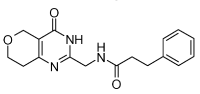	5.6	18.7	-	-	>50	-0.91	0.25
23	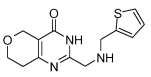	7.2	2.93	-	-	>50	-1.6	0.58
24	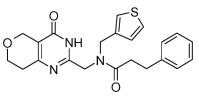	5.6	1.03	71.2	10.4	8.54	0.42	0.96

[a]LipE = pIC_{50} (TNKS2) − clogP. [b]HEK293 SuperTopFlash reporter gene assay. [c]Rat liver microsome extraction ratio. [d]Measured log *D*. [e]LipE = pIC_{50} (TNKS2) − log *D*.

Scheme 3. Synthesis of Dihydropyran C-Ring Analogues[a]

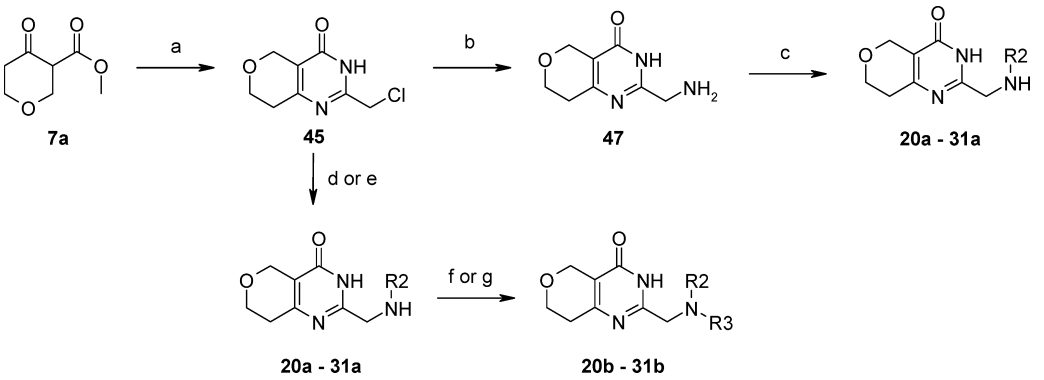

[a](a) TEA, 2-chloroacetamidine, MeOH; (b) i. NaN_3, H_2O/acetone, ii. Ph_3P, THF; (c) R^2-CHO, $SiCNBH_3$, AcOH, EtOH; RSO_2Cl, TEA, DCM or RCO_2Cl, TEA, DCM or RCO_2H, EDCI, HOBt, TEA, DCM; (d) i. $BocNHR^2$, NaH, THF or DMF; ii. HCl, dioxane, MeOH; (e) R_3NH_2, TEA, 120 °C, 5 min, or R_3NH_2, TEA or DIEA, EtOH, 65 °C; (f) RCO_2Cl, TEA, DCM; (g) RCO_2H, EDCI, HOBt, TEA, DCM.

but microsomal stability remained low. We began by stepwise deletion of the thiophene and the phenpropanamide moieties to investigate their importance in binding efficiency and microsomal stability with the synthesis of this series described in Scheme 3. Truncation to the *N*-ethyl derivative **21** or to the secondary amide **22** resulted in lower binding efficiency and cellular activity but improved microsomal stability. Deletion of the amide moiety (**23**) also improved microsomal stability but also increased LipE significantly, suggesting this was an inefficient binding motif. The 3-thiophenyl analogue **24** was 5-fold less active, and activity was lost with other linker modifications (data not shown).

We next kept the thiophene constant and surveyed analogues of the amide group (Table 4). Examination of the crystal structure of **19** suggested that there were potential polar interactions that might be gained, as the hydroxyl of Ser1186 and the backbone carbonyl of D1198 were in close proximity to the phenyl ring (Figure 2). Additionally, a crystallographic water molecule was bound via the backbone NH of D1198, and we sought to make a hydrogen bond with this water molecule. Both compounds **25** and **26** were less potent than **20**; however, **25** had significantly improved LipE. For a ΔclogP of −1.52, both analogues would be expected to be about 33-fold less potent than **20** from a LipE perspective. Compound **25** maintains similar LipE and is 37-fold less potent, and the in vitro stability improves somewhat, presumably because of the lower lipophilicity. For analogue **26**, however, the 4-fold decrease in potency is much better than the expected 33-fold drop and is consistent with the formation of a hydrogen bond with the bound water. Fluorine derivatives (**27**−**29**) were tested, and compounds **27** and **29** were both more potent and had improved LipE, however were unstable in microsomes. We

dx.doi.org/10.1021/jm400807n | J. Med. Chem. XXXX, XXX, XXX−XXX

Table 4. Structure–Efficiency Relationships of Tribrid Phenpropyl Amide Analogues

Compound	Structure	TNKS2 LipE[a]	IC_{50} (μM) TNKS2	PARP2	STF[b]	clogP	RLM ER[c]
20	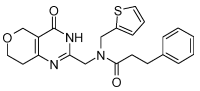	6.2	0.216	56.4	1.92	0.42 2.15[d]	0.95
25	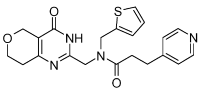	7.1	0.958	-	8.25	-1.1	0.81
26	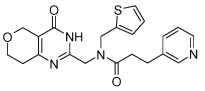	6.1	7.96	-	41.0	-1.1	0.85
27	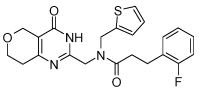	6.6	0.064	-	0.304	0.56	0.96
28	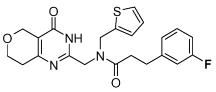	6.0	0.284	-	6.61	0.56	-
29	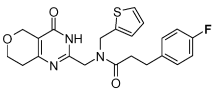	6.5	0.078	-	0.483	0.56	>0.97
30	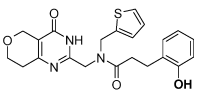	6.4	0.766	-	3.77	-0.30	-
31	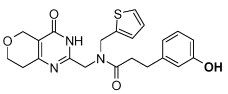	7.0	0.180	>19	0.812	-0.25	0.88
32	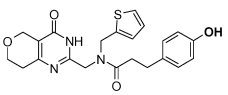	6.7	0.345	-	1.35	-0.25	-

[a]LipE = pIC_{50} (TNKS2) − clogP. [b]HEK293 SuperTopFlash reporter gene assay. [c]Rat liver microsome extraction ratio. [d]Measured log *D*. [e]LipE = pIC_{50} (TNKS2) − log *D*.

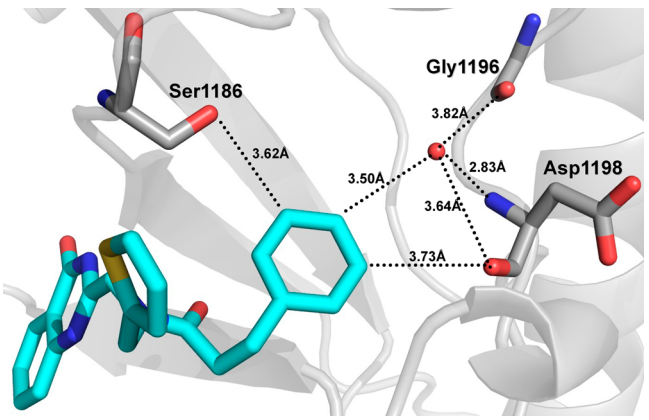

Figure 2. Crystal structure of **19** (pdb 4LI6) suggested potential polar interactions that might be gained, as (1) the hydroxyl of Ser1186 and the backbone carbonyl of D1198 were in close proximity to the phenyl ring and (2) a crystallographic water molecule was bound via the backbone NH of D1198.

next sought to replace the structural water with hydroxyl substituents to make direct interactions with Asp1198. Each of these analogues are more polar than **20** (ΔclogP = −0.7), and therefore because of the desolvation penalty these analogues would be expected to be less potent unless a compensating hydrogen bond was made. Although compound **30** is less active than **20** but with similar LipE, compounds **31** and **32** have similar biochemical activity and increased LipE relative to **20**. In the case of **31** we speculate that the increased LipE may be diagnostic of the formation of a hydrogen bond with the TNKS protein, and the strength of this hydrogen bond is of similar strength to that which was lost upon desolvation. From this subset of compounds, we concluded that more specific interactions with the TNKS protein and improved cellular activity were possible, but the thiophene remained a key liability that needed to be addressed. Yet again a more dramatic change to the structure was needed, and we focused on completely replacing the phenethyl moiety because of its low contribution to the overall LipE of the scaffold.

Our screening and structural biology efforts identified a diverse range of TNKS binders such as **1**, which bound to the nicotinamide pocket,[249] compounds which bound exclusively to the adenosine pocket,[9] and also compounds, such as **33**,[27] which simultaneously occupied the nicotinamide and adenosine pockets (Figure 3). A crystal structure of TNKS1 in complex with **33** was determined to 2.2 Å resolution to understand the binding mode. For this compound, a cyanobenzamide sits in place of the A and B rings of **1** with the nitrile group forming polar interactions with the hydroxyl of Ser1221 and the backbone amide of Gly1185. Compound **33** extends through the diphosphate binding region and reaches into the adenosine pocket where the fluorophenyl group forms van der Waals interactions with the side chains of Phe1188, Ala1191, and Ile1192 on one side of the groove, and a stacking interaction with the side chain of His1201 on the opposite side. A

dx.doi.org/10.1021/jm400807n | J. Med. Chem. XXXX, XXX, XXX–XXX

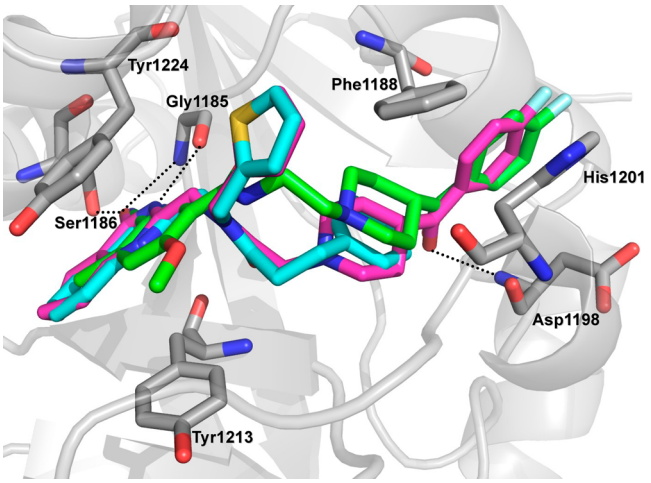

Figure 3. Superposition of crystal structures **19** (pdb 4LI6, cyan), **33** (pdb 4LI7, green), and **35** (pdb 4LI8, magenta) bound to TNKS1. Grafting of the nicotinamide/nook binding portion of **19** with the adenosine binding portion of **33** led to **35**, the first known three-pocket tankyrase binder, a compound with excellent potency, highly favorable physicochemical properties, and metabolic stability.

hydrogen bond is also formed between **33** and the backbone amide of Asp1198.

Relative to **1** and **20**, compound **33** has much lower LipE but has moderate biochemical and cellular activity. The cyanobenzamide represented another novel nicotinamide isostere that we found in our screens, and we hypothesized that if we retained the high LipE fragment **23** it might be possible to find improvements by grafting on a new substructure, such as the (4-fluorophenyl)piperidin-4-ylmethanone moiety of **33**. The synthesis of these analogues was accomplished following the approach outlined in Scheme 4. To our great satisfaction, the first two hybrid molecules based on this design (Table 5, **34** and **35**) had excellent potency, substantially improved LipE, and, in the case of **34** (LipE = 6.6 based on measured log *D*), highly favorable physicochemical properties and metabolic stability. While recent examples exist of compounds that bind in the nicotinamide and adenosine pockets,[16] or to the adenosine and "nook" pockets,[18,28] to our knowledge, this is the first example of a tankyrase inhibitor that binds simultaneously to the nicotinamide, adenosine, and "nook" pockets. We benchmarked these compounds in multiple in vitro and in vivo assays while further optimization continued.

The oral and intravenous pharmacokinetics of **34** and the *N*-methylthiophene analogue, **35**, were evaluated in mice. After intravenous administration, both compounds showed low CL with a moderate volume of distribution. **34** was given orally over a dose range from 5 to 800 mg/kg as a solution (5 and 25 mg/kg) or a suspension (200−800 mg/kg) dose. **34** exhibited good oral exposure with a bioavailability of 40−60% over the dose range. The exposure was slightly overproportional over the range as evidenced by the dose normalized AUC's ranging from 400 to 704 for the 5 and 800 mg/kg doses, respectively. The oral pharmacokinetics of **35** was evaluated as a solution dose of 30 and 100 mg/kg. **35** showed significantly lower oral exposure as a result of the lower oral bioavailability of approximately 12%.

We explored various substitution patterns on the thiophene (Table 5), none of which improved the microsomal stability or improved potency. The benzyl derivative (**36**) had a very slight improvement in microsomal stability, however lost 18-fold activity in the cellular assay. The heterocyclic replacements (e.g., **37**) had improvements in LipE, but as was the case for compounds **13**, **14**, **16** and **17**, these modifications are solvent-exposed, modulate compound properties but do not represent any improvement in binding efficiency to TNKS. We then moved away from aromatic ring systems and then looked at a series of alkyl substituents (**38**−**41**). For these analogues LipE appeared inversely correlated with the bulkiness of the alkyl substituent. Another trend appeared that rat liver microsomal extraction ratio (rLMER) decreased as the compounds became less lipophilic. Compounds **40** and **41** had a good combination of LipE, potency, and rLMER. Because **38** was the most potent of the alkyl derivatives, the *N*-cyclopropylmethyl analogue **42** was made and found to be equipotent but with improved rLMER. The oral exposure of compound **42** in rat was 10-fold greater than **34** (data not shown) and represented a suitable thiophene replacement to enable further in vivo studies. Turning once again to our structural data from our previously reported TNKS inhibitor which binds exclusively to the adenosine binding pocket, we noted that the fluorophenyl ring of **34** is in close proximity to the methoxyphenyl ring of **2** (Figure 4) and, despite not being an exact overlay, we wondered if the methoxy would be a more favorable substituent because the methoxy group significantly improved LipE in the previous series.[9] Replacing the fluorine of **42** with a methoxy group led to TNKS656 (compound **43**) that was a highly potent and efficient inhibitor of TNKS1&2 (LipE = 7.0 based on measured log *D*), with over 5,000-fold selectivity versus

Scheme 4. [a]

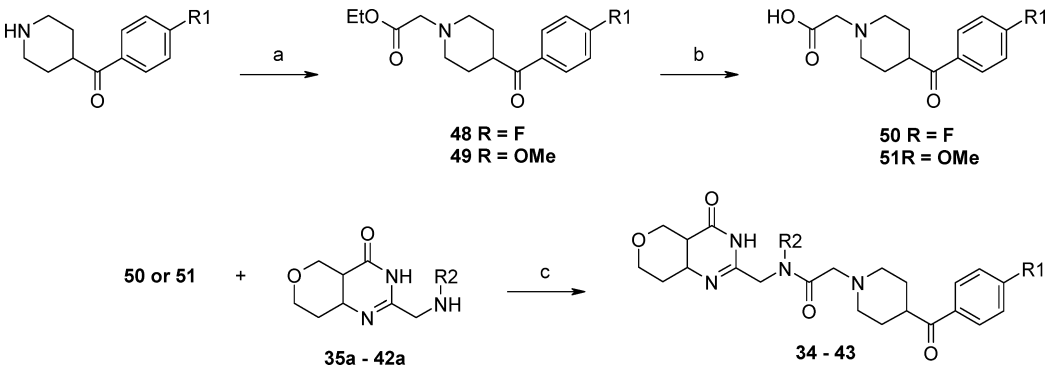

[a](a) Ethyl 2-bromoacetate, Et_3N, CH_3CN, reflux 5 h; (b) NaOH, H_2O, EtOH, 24 h; (c) EDCI, HOBt or HATU, TEA or DIPEA, DCM or DMF.

dx.doi.org/10.1021/jm400807n | J. Med. Chem. XXXX, XXX, XXX−XXX

Table 5. Incorporation of Compound 33 into the Design of Three-Point Binders

Compound	Structure	TNKS2 LipE[a]	IC_{50} (μM) TNKS2	PARP1	PARP2	STF[b]	clogP	RLM ER[c]
33	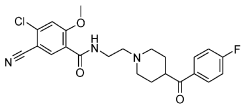	2.8	0.770	>19	-	1.10	3.5	0.85
34	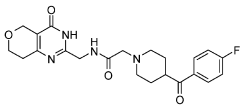	8.9 6.6[e]	0.023	10.4	3.15	0.040	-1.1 1.2[d]	0.16
35	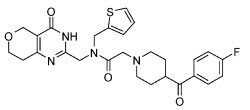	7.7	0.0075	0.142	>19	0.0036	0.47	0.93
36	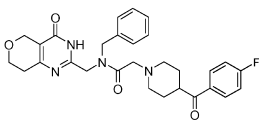	7.0	0.016	>19	>19	0.065	0.84	0.93
37	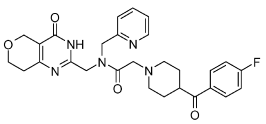	8.2	0.031	>19	>19	0.052	-0.67	0.84
38	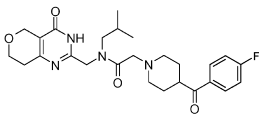	7.0	0.018	>19	>19	0.017	0.76	0.88
39	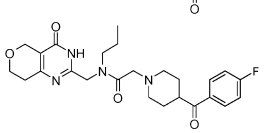	7.6	0.011	>19	>19	0.034	0.36	0.69
40	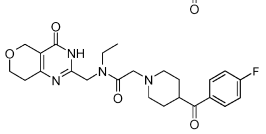	7.6 6.3[e]	0.035	>19	>19	0.070	-0.17 0.73[d]	0.48
41	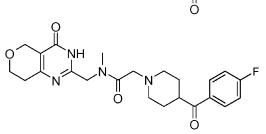	7.9	0.057	-	-	0.193	-0.70	0.48
42	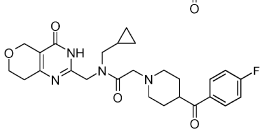	7.9 6.8[e]	0.011	-	-	0.017	0.16 1.3[d]	0.65
43 **TNKS656**	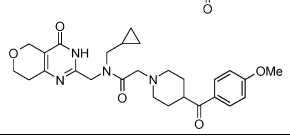	8.1 7.0[e]	0.0060	>19	32	0.0035	0.16 1.3[d]	0.50

[a]LipE = pIC_{50} (TNKS2) − clogP. [b]HEK293 SuperTopFlash reporter gene assay. [c]Rat liver microsome extraction ratio. [d]Measured log *D*. [e]LipE = pIC_{50} (TNKS2) − log *D*.

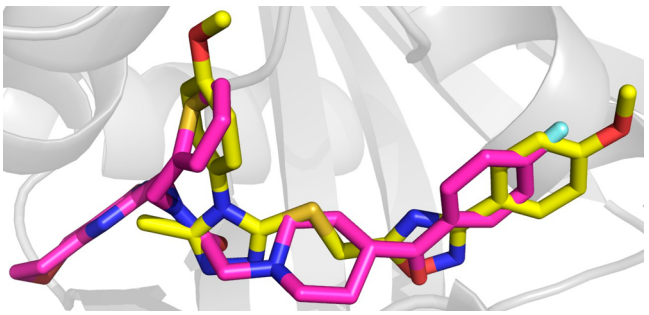

Figure 4. Superposition of the crystal structures of **35** (pdb 4LI8, magenta) and **2** (pdb 3UDD, yellow).

PARPs 1 and 2. With low to moderate microsomal ER values across species and high solubility, compound **43** was progressed into advanced in vivo studies.

To assess the potential for in vivo inhibition of Tankyrase signaling by **43**, we first examined the pharmacokinetics in mice (Table 6). After intravenous administration, **43** displayed low clearance and volume of distribution (V_{Dss}) (10 mL/min/kg and 0.6 L/kg, respectively). After oral administration of either a 30 or 100 mg/kg dose, **43** exhibited good exposure and moderate oral bioavailability of 32% and 53%, respectively. Some slight overproportional increase in oral exposure was observed between 30 and 100 mg/kg with the dose normalized AUC for the 100 mg/kg dose being 2-fold higher than for the

dx.doi.org/10.1021/jm400807n | J. Med. Chem. XXXX, XXX, XXX−XXX

Table 6. Mouse Pharmacokinetic Properties of Compound 43

		po	
	iv, 1 mg/kg	30 mg/kg	100 mg/kg
AUC (μM·h)	3.46	33.4	183.4
CL (mL/min/kg)	9.7		
$T1/2$ (h)	1.3		
V_{dss} (L/kg)	0.6		
C_{max} (μM)		16.8	79.7
T_{max} (h)		0.4	0.8
F (%)		32	53

30 mg/kg dose. With a cell potency of 3.5 nM and a free fraction of 16% in mouse from rapid equilibrium dialysis, **43** should have unbound drug concentrations exceeding the IC_{50} for at least 12 h.

To investigate the in vivo PK/PD activity of **43**, we utilized mammary adenocarcinomas derived from the mouse mammary tumor virus (MMTV)-Wnt1 transgenic model resulting in Wnt signaling activation (Figure 5).[29] Tumor fragments from these

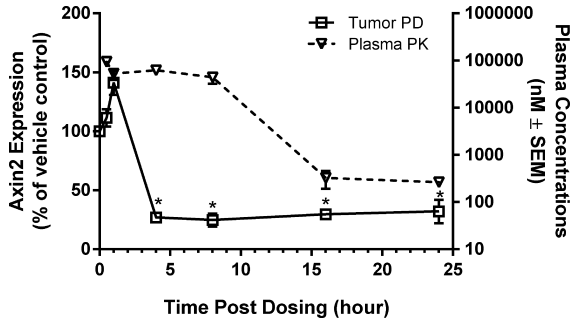

Figure 5. PK/PD relationship of **43** in MMTV-Wnt1 tumor bearing athymic nude mice. Following a single oral dose of **43** at 350 mg/kg, plasma and tumor samples were collected at various time points (0.5, 1, 2, 4, 8, 16, and 24 h; $n = 3$) for PK and PD analysis. The data are represented as **43** concentration in plasma (nM) and %Axin2 mRNA in tumor relative to untreated controls (mean ± SEM, $n = 3$ animals/time point). $p < 0.05$ compared to untreated controls using a one-way ANOVA followed by a posthoc Tukey test.

mice were allografted subcutaneously into recipient nude mice and grown to approximately 250−300 mm.[3] To determine if **43** could modulate Wnt/beta-catenin signaling, cohorts of MMTV-Wnt1 tumor bearing mice ($n = 3$) were treated with either vehicle or a single oral dose of **43** at 350 mg/kg over a 24-h time course. Mice treated with **43** showed good plasma and tumor exposures corresponding to AUC_{0-24h} of 515 and 325 μM·h, respectively. Consistent with the proposed mechanism of action of TNKS inhibition, **43**-treated tumors showed a stabilization of Axin1 protein (data not shown) and a corresponding 70−80% reduction in the Wnt/beta-catenin target gene Axin2 mRNA level compared to vehicle control animals. The decrease in Axin2 mRNA expression was detected as early as 4 h post treatment and persisted through the 24 h time course, suggesting once daily dosing may be sufficient for sustained target inhibition. Additional studies will be needed to further model the dose−effect relationship in this model.

The thermodynamics of inhibitor binding, especially enthalpy of binding, has been identified as an important factor in identifying quality compounds.[30] Using isothermal calorimetry (ITC), we measured the thermodynamic signature of select analogues from the optimization process to determine what effect the optimization had on the thermodynamics of binding (Supporting Information Table 1, Figure 6). Karlberg

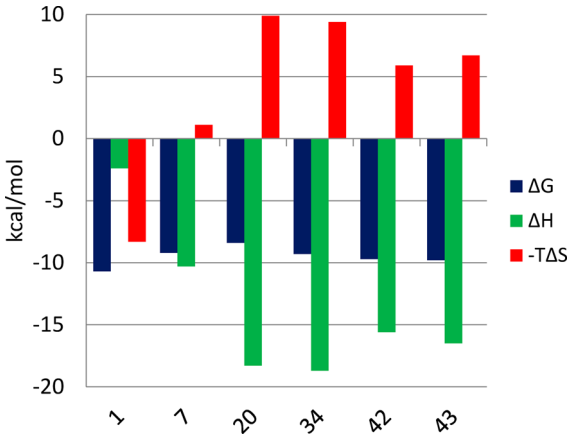

Figure 6. Isothermal calorimetry data for select compounds.

et al. determined that **1** binds with both favorable enthalpic and entropic contributions, although entropic contributions are more significant.[32] Compound **7**, despite having TNKS2 affinity lower than that of **1**, has a similar LipE, but binding is enthalpy-driven ($\Delta H = -10.3$ kcal/mol) with a slight entropic penalty ($T\Delta S = -1.1$ kcal/mol). Compound **20** was the first analogue that went beyond the ABC ring system of XAV939 and was only 3-fold less potent than **7**. The improved thermodynamic profile ($\Delta H = -18.3$ kcal/mol) is likely due in part to the additional hydrogen bond gained to the amide carbonyl. **20** has a secondary amide bond in the linker, and therefore we hypothesize a portion of the large unfavorable entropic penalty ($T\Delta S = -9.9$ kcal/mol) must be paid for the s-cis amide conformation to bind. Further optimization into the hybrid **34** benefits from an additional hydrogen bond ($\Delta H = -18.7$ kcal/mol) while the entropic penalty is only slightly diminished. The potency gain with **42** is attributed to potency gained from desolvation of the hydrophobic cyclopropylmethyl moiety, while the terminal methoxy group of **43** again shifts to a more enthalpy-driven binding signature. The high enthalpy of binding is reflected in the high selectivity of this class of compounds against PARPs 1 and 2 as well as a panel of off-target activities (data not shown).

CONCLUSION

We previously reported the identification of novel inhibitors of TNKS which is a druggable node in the Wnt pathway. Beginning with compound **1**, we explored the previously untested approach of utilizing LipE to survey a diverse range of chemical structures to understand what portions of each molecule efficiently interacted with our target protein. With this information we undertook a LipE-driven optimization approach at several junctures. We consciously deprioritized modifications to achieve more potent compounds in favor of modifications to obtain less potent, but more lipophilic, efficient inhibitors. We went from compound **1** (cellular IC_{50} of 0.078 μM) to compound **7** (cellular IC_{50} of 2.7 μM) to compound **20** (cellular IC_{50} of 1.9 μM) before finally optimizing to **43** (cellular IC_{50} of 0.0035 μM) with demonstrated in vivo activity for proof of concept studies. The thermodynamic profile of key analogues generated during the optimization demonstrates that

dx.doi.org/10.1021/jm400807n | J. Med. Chem. XXXX, XXX, XXX−XXX

our optimization created inhibitors with enthalpy-driven binding. It is possible that a LipE-driven optimization approach may be a more general approach for yielding enthalpy-driven inhibitors, but further studies investigating this are warranted. For the case of TNKS, LipE was a valuable decision-making tool for the rapid generation of potent, selective, and in vivo active compounds for target validation and lead optimization.

MATERIALS AND METHODS

Tankyrase AutoPARsylation Assay. PARP catalytic activity was monitored using the quantitative liquid chromatography/mass spectrometry (LC-MS) detection of nicotinamide, as previously described.[7] The autoPARsylation reactions were performed at room temperature in 384-well Greiner flat-bottom plates. The final reaction mixture contained 2.5% DMSO and inhibitors with concentrations ranging from 0.0001 to 18.75 μM. GST-TNKS2P, GST-TNKS1P, PARP1, and PARP2 enzymes were used at final concentrations or 5, 5, 5, and 2 nM, respectively. The nicotinamide concentration in the resulting supernatants was measured by LC-MS. The % inhibition was calculated as follows: (control − sample)/(control − background) × 100. "Control" is the average value of eight wells without compound, and "background" is the average of eight wells mixed with 5× quenching solution measured prior to initiation of the reaction.

SuperTop Flash (STF) Reporter Gene Assay. Compound activity in inhibiting Wnt ligand-induced signaling was measured using a Wnt-responsive SuperTopFlash (STF) luciferase reporter gene assay in HEK293 cells. The % inhibition was calculated as follows: (maximum Wnt-induced signaling − sample)/(maximum Wnt-induced signaling − background) × 100. "Maximum Wnt-induced signaling" is the STF signal level induced by 20% Wnt3A CM without compound, and "background" is the STF signal level without the addition of Wnt3A CM or compound. To demonstrate the specific activity of inhibitors regulating Wnt signaling, counter screen was performed in HEK293T cells expressing a cAMP-response element (CRE) luciferase reporter gene. Compound activity on the CRE-reporter was measured in the presence of 10 μM forskolin, which is an activator of cAMP signaling.

Axin2 Protein ELISA. Compound activity in stabilizing the Axin2 protein was measured by Sandwich enzyme-linked immunosorbent (ELISA) assay in the colorectal cell line SW480. Cell lysates were prepared from cells treated with compounds in six-point dilution starting at 10 μM for 24 h. For the ELISA assay, anti Axin-2 capture antibody was diluted to a concentration of 1 μg/mL (1:1000) in carbonate coating buffer, pH 9.2 (Sigma, C3041−50CAP). Then 100 μL of the diluted anti Axin-2 capture antibody per well was used to coat the 96-well plate overnight at 4 °C. Plates were then washed three times with wash solution, PBST20 (PBS + 0.05% Tween), and blocked with 1% BSA/PBS for 1.5 h at room temperature while shaking gently. After blocking, plates were then washed three times with wash solution. Then 100 μL of prepared SW480 cell lysate was added to each well and incubated at room temperature for 2 h while shaking gently. After washing, 100 μL of biotinylated anti-Axin2 antibody was added to each well and incubated at room temperature for 2 h. Signal was detected by chemiluminescence (Pierce SuperSignal ELISA Femto no. 3704) using streptavidin-HRP (R&D Systems, DY998) and measured on PerkinElmer Wallac 1420 plate reader.

MMTV-Wnt1 Allograft Model. Athymic female nude mice (Harlan Laboratories) weighing 19−22 g were implanted subcutaneously with a 3 × 3 × 3 mm^3 tumor fragment from an MMTV-Wnt1 tumor-bearing mouse. Tumors were grown to approximately 250−300 mm^3. Individual mice were given a single oral dose of vehicle (n = 3) (4% HCl:10% propylene glycol:20% Solutol HS15:60.5% D5W:0.5% NaOH) or TNKS656 at 350 mg/kg (n = 18). At 0.5, 1, 2, 4, 8, 16, or 24 h following dosing (n = 3/time point), mice were euthanized, and blood was collected via cardiac puncture and processed for plasma. Tumors were excised from mice and frozen at −80 °C for PD analysis.

Protein Purification and Crystallization. Human TNKS1 protein was expressed, purified, and crystallized as previously described.[24] To obtain crystals containing either **19**, **33**, or **35**, TNKS1/PJ34 complex crystals were transferred into a soaking solution containing 100 mM Bis-Tris pH 5.8, 18% PEG 3350, 320 mM ammonium sulfate, and 200 μM of compound. Transfer of the crystals into fresh solution occurred once per hour over a 4 h period. Crystals were cryoprotected using the same soaking solution with the addition of 20% glycerol, followed by flash-freezing directly into liquid nitrogen.

Data Collection and Structure Determination. Diffraction data for the TNKS1/**19** complex were collected on a Saturn92 CCD Detector using Cu Kα radiation (λ = 1.5418 Å) from a Rigaku FR-E rotating anode X-ray generator operating at 45 mV and 45 mA. Diffraction data for the TNKS1/**33** complex were collected on a Quantum315R CCD Detector at the ALS beamline BL5.0.3 at a wavelength of 1 Å. Diffraction data for the TNKS1/**35** complex were collected on a Dectris Pilatus 6 M Detector at the Swiss Light Source beamline X06SA at a wavelength of 1 Å. The data were measured from a single crystal, and the reflections were indexed, integrated, and scaled using XDS and XSCALE[29] or HKL2000.[25] The space group of the complex was C2 with two molecules in the asymmetric unit. The structure was determined with Fourier methods, using the TNKS1/PJ34 structure (pdb 3UH2) with active site waters and inhibitors removed as the starting model.

Structure determination was achieved through iterative rounds of positional and simulated annealing refinement using CNX[26] or PHENIX[27] with model building using COOT[28] Individual B-factors were refined, and a bulk solvent correction was applied. The solvent, sulfate ions, and inhibitor were built into the density in later rounds of the refinement. Data collection and refinement statistics are shown in Supporting Information Table 2.

Isothermal Calorimetry. Isothermal calorimetry was used to determine the thermodynamic properties of ligand binding. Data were collected at 25 °C on an Auto-iTC$_{200}$ (GE Healthcare) using a sample buffer of 25 mM HEPES pH 7.4, 150 mM NaCl, with a matched DMSO concentration between the titrant and cell. Direct titration of 200 μM compound into 20 μM TNKS1 over 16 injections of 2.5 μL was performed in the case of **34**, **42**, and **43**. Direct titration of 300 μM compound into 20 μM TNKS1 over 20 injections of 2 μL was performed in the case of **20**. Finally, a reverse titration using 200 μM TNKS1 into 20 μM **7** over 16 injections of 2.5 μL was performed. The individual heat values were plotted against the molar ratio, and the values for the number of binding sites (n), the enthalpy change (ΔH), and dissociation constant (K_D = $1/K_A$) were obtained by nonlinear regression of the data.

Chemical Synthesis. The purity of all compounds was determined using high resolution HPLC/MS characterization and found to be >95% pure except as noted. High resolution LC/ESI-MS data were recorded using an Agilent 6220 mass spectrometer with electrospray ionization source and an Agilent 1200 liquid chromatograph with a gradient from 5% to 95% acetonitrile in water on a C18 reverse phase column with a diode array detection. The resolution of the MS system was approximately 11000 (fwhm definition). HPLC separation was performed using one of the methods (denoted in the header text) listed at end of report. Purine and hexakis(1*H*,1*H*,3*H*-tetrafluoropropoxy)phosphazine (protonated molecules m/z 121.05087 and 922.00979, respectively) were used as a reference. The mass accuracy of the system has been found to be <2 ppm.

*General Procedure A: Synthesis of Benzamidines. 4-(Trifluoromethoxy)benzimidamide (**15a**).* Trimethylaluminum (2 M in toluene, 2.4 mL, 4.8 mmol, 3 equiv) was added to a ca. 5 °C suspension of ammonium chloride (257 mg, 4.8 mmol, 3 equiv) in 8 mL of toluene. The reaction mixture was then stirred in the cold bath for 1.5 h and then at room temperature for 0.5 h. 4-(Trifluoromethoxy)benzonitrile (300 mg, 1.6 mmol, 1.0 equiv) was then added, and the reaction mixture was heated to reflux overnight. The reaction mixture was cooled to room temperature, quenched with MeOH (30 mL), and cooled in an ice bath, and 2 g of silica gel in DCM with 1% MeOH was added. The mixture was stirred for 15 min, and the solid was collected and then washed with excess MeOH. The filtrate was concentrated in vacuo to give a white solid (327 mg, 1.6 mmol, 100% yield) and used without further purification.

dx.doi.org/10.1021/jm400807n | J. Med. Chem. XXXX, XXX, XXX−XXX

*General Procedure B: Synthesis of Pyrimidinones. 2-(4-(Trifluoromethyl)phenyl)-7,8-dihydro-3H-thiopyrano[4,3-d]-pyrimidin-4(5H)-one (**1**).* K_2CO_3 (1.42 g, 10.2 mmol, 2.0 equiv) was added to a room temperature mixture of methyl 4-oxotetrahydro-2*H*-thiopyran-3-carboxylate[31] (876 mg, 5.03 mmol) and 4-(trifluoromethyl)benzimidamide hydrochloride dihydrate (1.42 g, 5.46 mmol, 1.08 equiv) in methanol (25 mL). The reaction mixture was then refluxed overnight. The reaction mixture was then filtered with the aid of methanol and then concentrated to ca. 1/4 volume. The resulting material was dissolved in water and acidified to ca. pH 3 using 1 N aqueous HCl. The resulting precipitate was filtered and washed several times with water/MeOH (1:1) followed by several washes with ether. The resulting white solid was dried in a high vacuum oven (35 °C) for several hours, affording **1** (1.24 g, 79%) as a white solid. Exact mass calculated for $C_{14}H_{12}F_3N_2OS$ 313.0622, found 313.0628 (ESI, M + H). 1H NMR (400 MHz, DMSO-d_6) δ ppm 12.94 (br s, 1 H) 8.28 (d, J = 8.08 Hz, 2 H) 7.89 (d, J = 8.59 Hz, 2 H) 3.55 (s, 2 H) 2.91 (s, 4 H)

*Ethyl 3-Oxotetrahydro-2H-thiopyran-2-carboxylate (**3a**).* One drop of MeOH was added to a room temperature suspension of NaH in Et_2O (2 mL). A solution of ethyl 4-((2-ethoxy-2-oxoethyl)-thio)butanoate in Et_2O (4 mL) was then added, and the reaction mixture was heated at reflux for 5 h. The reaction mixture was cooled to room temperature and then quenched with 3 N aq AcOH. After separation, the aqueous layer was extracted with Et_2O (2 × 80 mL). The combined organic layers were washed several times with sat. $NaHCO_3$ solution, dried over $MgSO_4$, filtered, and concentrated in vacuo to dryness affording ethyl 3-oxotetrahydro-2*H*-thiopyran-2-carboxylate as a brown oil which was used without further purification. Mass calculated for $C_{14}H_{11}F_3N_2OS$ 312.1, found 313.0 (ESI, M + H). ^{1}H NMR (400 MHz, DMSO-d_6) δ ppm 12.94 (br s, 1H), 8.26 (d, J = 8.1 Hz, 2H), 7.87 (d, J = 8.6 Hz, 2H), 2.99 (td, J = 2.9, 5.3 Hz, 2H), 2.76 (t, J = 6.1 Hz, 2H), 2.14−2.01 (m, 2H).

*2-(4-(Trifluoromethyl)phenyl)-7,8-dihydro-3H-thiopyrano[3,2-d]-pyrimidin-4(6H)-one (**3**).* Following general procedure B, the title compound (64 mg, 0.21 mmol, 29% yield) was prepared from ethyl 3-oxotetrahydro-2*H*-thiopyran-2-carboxylate (142 mg, 0.72 mmol, 1.0 equiv) and 4-(trifluoromethyl)benzimidamide (200 mg, 0.77 mmol, 1.1 equiv). Mass calculated for $C_{14}H_{11}F_3N_2OS$ 312.1, found 313.0 (ESI, M + H). ^{1}H NMR (400 MHz, DMSO-d_6): δ 12.94 (br s, 1H), 8.26 (d, J = 8.1 Hz, 2H), 7.87 (d, J = 8.6 Hz, 2H), 2.99 (td, J = 2.9, 5.3 Hz, 2H), 2.76 (t, J = 6.1 Hz, 2H), 2.14−2.01 (m, 2H).

*2-(4-(Trifluoromethyl)phenyl)-4a,5,7,7a-tetrahydrothieno[3,4-d]-pyrimidin-4(3H)-one (**4**).* Following general procedure B, the title compound (14.7 mg, 0.05 mmol, 9% yield) was prepared from methyl 4-oxotetrahydrothiophene-3-carboxylate (95 mg, 0.56 mmol, 1.0 equiv) and 4-(trifluoromethyl)benzimidamide hydrochloride dihydrate (200 mg, 0.62 mmol, 1.1 equiv). Mass calculated for $C_{13}H_9F_3N_2OS$ 298.04, found 299.0 (ESI, M + H). ^{1}H NMR (400 MHz, DMSO-d_6) δ ppm 13.02 (br s, 1H), 8.29 (d, J = 7.6 Hz, 2H), 7.90 (d, J = 8.6 Hz, 2H), 4.23 (d, J = 3.0 Hz, 2H), 4.05 (d, J = 3.0 Hz, 2H).

*2-(4-(Trifluoromethyl)phenyl)-5,6,7,8-tetrahydroquinazolin-4(3H)-one (**5**).* Following general procedure B, the title compound (53 mg, 0.18 mmol, 62% yield) was prepared from ethyl 2-oxocyclohexanecarboxylate (52 mg, 0.29 mmol, 1.0 equiv) and 4-(trifluoromethyl)-benzimidamide hydrochloride dihydrate (100 mg, 0.38 mmol, 1.3 equiv). Exact mass calculated for $C_{15}H_{13}F_3N_2O$ 294.1, found 295.1 (ESI, M + H). ^{1}H NMR (400 MHz, DMSO-d_6): δ ppm 12.73 (br s, 1H), 8.28 (d, J = 7.6 Hz, 2H), 7.87 (d, J = 8.1 Hz, 2H), 2.70−2.57 (m, 2H), 2.42 (br s, 2H), 1.83−1.63 (m, 4H).

*N-(2-Carbamoylphenyl)-4-(trifluoromethyl)benzamide (**6a**).* In a 20 mL vial, 4-(trifluoromethyl)benzoyl chloride (184 mg, 0.88 mmol, 1.2 equiv) was added to 2-aminobenzamide (100 mg, 0.73 mmol, 1.0 equiv) and DIEA (192 uL, 1.1 mmol, 1.5 equiv) in THF, and the reaction was stirred for 2 h resulting in a white precipitate. The reaction mixture was diluted with heptane, and the solid was collected, triturated with water, collected again, and then air-dried to give a white solid. The title compound (226 mg, 0.733 mmol, 100% yield) was used without further purification. Mass calculated for $C_{15}H_{11}F_3N_2O_2$ 308.1, found 309.1 (ESI, M + H). ^{1}H NMR (400 MHz, DMSO-d_6) δ 13.13 (s, 1H), 8.68 (d, J = 8.59 Hz, 1H), 8.44 (br s, 1H), 8.13 (d, J = 8.08 Hz, 2H), 7.98 (d, J = 8.59 Hz, 2H), 7.92 (dd, J = 1.26, 7.83 Hz, 1H), 7.82−7.89 (m, 1H), 7.55−7.63 (m, 1H), 7.17−7.25 (m, 1H).

*2-(4-(Trifluoromethyl)phenyl)quinazolin-4(3H)-one (**6**).* In a 5 mL microwave vial, *N*-(2-carbamoylphenyl)-4-(trifluoromethyl)benzamide (226 mg, 0.73 mmol, 1.0 equiv) and KOEt (123 mg, 1.46 mmol, 2.0 equiv) were heated in the microwave at 140 °C for 20 min. The mixture was poured into 1 N HCl, and the resulting white solid was collected, washed with heptane, and air-dried to provide the title compound (202 mg, 0.696 mmol, 95% yield). Mass calculated for $C_{15}H_9F_3N_2O$ 290.1, found 291.2 (ESI, M + H). ^{1}H NMR (400 MHz, DMSO-d_6) δ 12.73 (br s, 1H), 8.38 (d, J = 8.08 Hz, 2H), 8.18 (dd, J = 1.52, 8.08 Hz, 1H), 7.93 (d, J = 8.59 Hz, 2H), 7.84−7.90 (m, 1H), 7.77−7.81 (m, 1H), 7.54−7.60 (m, 1H).

*2-(4-(Trifluoromethyl)phenyl)-7,8-dihydro-3H-pyrano[4,3-d]-pyrimidin-4(5H)-one (**7**).* Following general procedure B, the title compound (190 mg, 35% yield) was prepared from methyl 4-oxotetrahydro-2*H*-pyran-3-carboxylate (290 mg, 1.83 mmol) and 4-(trifluoromethyl)benzimidamide hydrochloride dihydrate hydrochloride dihydrate (526 mg, 2.02 mmol). Mass calculated for $C_{14}H_{11}F_3N_2O_2$ 296.08, found 297.0 (ESI, M + H). ^{1}H NMR (400 MHz, DMSO-d_6) δ ppm 12.93 (br s, 1H), 8.29 (d, J = 8.08 Hz, 2H), 7.89 (d, J = 8.08 Hz, 2H), 4.46 (s, 2H), 3.91 (t, J = 5.56 Hz, 2H), 2.70 (br s, 2H).

*2-(4-(Trifluoromethyl)phenyl)-5,6-dihydro-3H-pyrano[3,4-d]-pyrimidin-4(8H)-one (**8**).* Following general procedure B, ethyl 3-oxotetrahydro-2*H*-pyran-4-carboxylate (100 mg, 0.436 mmol, 75% pure) and 4-(trifluoromethyl)benzimidamide (117 mg, 0.523 mmol) were converted to the title compound (82 mg, 0.277 mmol, 64% yield) as an off-white solid. MS m/z 297.2 (M + H), Ret time: 1.23 min; HRMS m/z (M + H) calculated for $C_{14}H_{11}F_3N_2O_2$: 297.0851, found: 297.0846. ^{1}H NMR (400 MHz, DMSO-d_6) δ 12.20−13.39 (m, 1H), 8.26 (d, J = 8.03 Hz, 2H), 7.90 (d, J = 8.03 Hz, 2H), 4.47 (s, 2H), 3.87 (t, J = 5.52 Hz, 2H), 2.50 (br s, 2H)

*2-(Thiophen-3-yl)-7,8-dihydro-3H-pyrano[4,3-d]pyrimidin-4(5H)-one (**9**).* Following general procedure B, methyl 4-oxotetrahydro-2*H*-pyran-3-carboxylate (100 mg, 0.474 mmol, 75% pure) and thiophene-3-carboximidamide (93 mg, 0.599 mmol) were converted to the title compound (73 mg, 0.296 mmol, 62% yield) as a yellow solid. MS m/z 235.2 (M + H), Ret time: 0.78 min; HRMS m/z (M + H) calculated for $C_{11}H_{10}N_2O_2S$: 235.0541, found: 235.0549. ^{1}H NMR (400 MHz, DMSO-d_6) δ 12.64 (br s 1H), 8.50 (s, 1H), 7.76 (d, J = 4.96 Hz, 1H), 7.66−7.70 (m, 1H), 4.41 (s, 2H), 3.88 (t, J = 5.51 Hz, 2H), 2.60−2.66 (m, 2H)

*2-(p-Tolyl)-7,8-dihydro-3H-pyrano[4,3-d]pyrimidin-4(5H)-one (**10**).* Following general procedure B, methyl 4-oxotetrahydro-2*H*-pyran-3-carboxylate (100 mg, 0.474 mmol, 75% pure) and 4-methylbenzimidamide (76 mg, 0.569 mmol) were converted to the title compound (40 mg, 0.165 mmol, 35% yield) as an off-white solid. MS m/z 243.3 (M + H), Ret time: 1.03 min; HRMS m/z (M + H) calculated for $C_{14}H_{14}N_2O_2$: 243.1134, found: 243.1138. ^{1}H NMR (400 MHz, DMSO-d_6) δ 12.65 (br s, 1H), 8.00 (d, J = 8.08 Hz, 2H), 7.33 (d, J = 8.08 Hz, 2H), 4.43 (s, 2H), 3.89 (t, J = 5.56 Hz, 2H), 2.66 (t, J = 5.31 Hz, 2H), 2.38 (s, 3H).

*2-(4-Chlorophenyl)-7,8-dihydro-3H-pyrano[4,3-d]pyrimidin-4(5H)-one (**11**).* Following general procedure B, methyl 4-oxotetrahydro-2*H*-pyran-3-carboxylate (100 mg, 0.474 mmol, 75% pure) and 4-chlorobenzimidamide (161 mg, 0.569 mmol) were converted to the title compound (80 mg, 0.283 mmol, 60% yield) as a yellow solid. MS m/z 263.2 (M + H), Ret time: 0.98 min; HRMS m/z (M + H) calculated for $C_{13}H_{11}ClN_2O_2$: 263.0587, found: 263.0587. ^{1}H NMR (400 MHz, DMSO-d_6) δ 12.61 (br s 1H), 8.11 (d, J = 8.82 Hz, 2H), 7.58 (d, J = 7.71 Hz, 2H), 4.42 (s, 2H), 3.89 (t, J = 5.51 Hz, 2H), 2.69−2.62 (m, 2H).

*2-(4-Bromophenyl)-7,8-dihydro-3H-pyrano[4,3-d]pyrimidin-4(5H)-one (**12**).* Following general procedure B, methyl 4-oxotetrahydro-2*H*-pyran-3-carboxylate (300 mg, 2.53 mmol, 75% pure) and 4-bromobenzimidamide (536 mg, 2.28 mmol) were converted to the title compound (183 mg, 0.554 mmol, 29% yield) as a white solid. MS m/z 307.1 (M + H), Ret time: 1.11 min; HRMS m/z (M + H)

dx.doi.org/10.1021/jm400807n | J. Med. Chem. XXXX, XXX, XXX−XXX

calculated for $C_{13}H_{11}BrN_2O_2$: 307.0082, found: 307.0070. ^{1}H NMR (400 MHz, DMSO-d_6) δ 8.03 (d, J = 8.46 Hz, 2H), 7.74 (d, J = 8.72 Hz, 2H), 7.25 (br s, 1H), 4.43 (s, 2H), 3.90 (t, J = 5.62 Hz, 2H), 2.67 (t, J = 5.31 Hz, 2H).

*2-(4-(Dimethylamino)phenyl)-7,8-dihydro-3H-pyrano[4,3-d]-pyrimidin-4(5H)-one (**13**).* Following general procedure B, ethyl 3-oxotetrahydro-2*H*-pyran-4-carboxylate (100 mg, 0.290 mmol, 50% pure) and 4-(dimethylamino)benzimidamide (76 mg, 0.348 mmol) were converted to the title compound (10 mg, 0.038 mmol, 13% yield) as a yellow solid. MS m/z 272.4 (M + H), Ret time: 1.05 min; HRMS m/z (M + H) calculated for $C_{15}H_{17}N_3O_2$: 272.1399, found: 272.1406. ^{1}H NMR (400 MHz, DMSO-d_6) δ 12.32 (br s, 1H), 8.00 (d, J = 9.03 Hz, 2H), 6.75 (d, J = 9.03 Hz, 2H), 4.40 (s, 2H), 3.79−3.92 (m, 2H), 3.00 (s, 6H), 2.61 (t, J = 5.27 Hz, 2H).

*2-(4-Methoxyphenyl)-7,8-dihydro-3H-pyrano[4,3-d]pyrimidin-4(5H)-one (**14**).* Following general procedure B, methyl 4-oxotetrahydro-2*H*-pyran-3-carboxylate (100 mg, 0.474 mmol, 75% pure) and 4-methoxybenzimidamide (85 mg, 0.569 mmol) were converted to the title compound (28 mg, 0.108 mmol, 23% yield) as an off-white solid. MS m/z 259.3 (M + H), Ret time: 0.97 min; HRMS m/z (M + H) calculated for $C_{14}H_{14}N_2O_3$: 259.1083, found: 259.1077. ^{1}H NMR (400 MHz, DMSO-d_6) δ 8.09 (d, J = 8.97 Hz, 2H), 7.0 (d, J = 8.97 Hz, 2H), 4.42 (s, 2H), 3.89 (t, J = 5.56 Hz, 2H), 3.84 (s, 3H), 2.62−2.67 (m, 2H).

*2-(4-(Trifluoromethoxy)phenyl)-7,8-dihydro-3H-pyrano[4,3-d]-pyrimidin-4(5H)-one (**15**).* Following general procedure B, the title compound (24 mg, 0.075 mmol, 16% yield) was prepared from **15a** (75 mg, 0.47 mmol, 1.0 equiv) and 4-(trifluoromethoxy)-benzimidamide (145 mg, 0.711 mmol, 1.5 equiv). Mass calculated for $C_{14}H_{11}F_3N_2O_3$ 312.2, found 313.1 (ESI, M + H). ^{1}H NMR (400 MHz, DMSO-d_6) δ 12.82 (br s, 1H), 8.21 (d, J = 7.58 Hz, 2H), 7.51 (d, J = 8.59 Hz, 2H), 4.44 (s, 2H), 3.90 (t, J = 5.56 Hz, 2H), 2.67 (br s, 2H).

*Methyl 4-(4-Oxo-4,5,7,8-tetrahydro-3H-pyrano[4,3-d]pyrimidin-2-yl)benzoate (**16**).* Following general procedure B, the title compound (601 mg, 80% yield) was prepared from methyl 4-oxotetrahydro-2*H*-pyran-3-carboxylate (402 mg, 2.63 mmol) and methyl 4-carbamimidoylbenzoate hydrochloride (0.672 g, 3.13 mmol). Mass calculated for $C_{15}H_{14}N_2O_4$ 286.29, found 287.2 (ESI, M + H). 1H NMR (400 MHz, DMSO-d6) δ ppm 12.86 (br s, 1H), 8.22 (d, J = 8.08 Hz, 2H), 8.07 (d, J = 8.59 Hz, 2H), 4.45 (s, 2H), 3.87−3.93 (m, 5H), 2.69 (br s, 2H).

*2-(4-(Methylsulfonyl)phenyl)-7,8-dihydro-3H-pyrano[4,3-d]-pyrimidin-4(5H)-one (**17**).* Following general procedure B, methyl 4-oxotetrahydro-2*H*-pyran-3-carboxylate (50 mg, 0.316 mmol) and 4-(methylsulfonyl)benzimidamide (89 mg, 0.379 mmol) were converted to the title compound (9 mg, 0.029 mmol, 9% yield) as white solid. MS m/z 307.3 (M + H), Ret time: 0.72 min; HRMS m/z (M + H) calculated for $C_{14}H_{14}N_2O_4S$: 307.0753, found: 307.0751. ^{1}H NMR (400 MHz, DMSO-d_6) δ 13.01 (br s, 1H), 8.30 (br s, 2H), 8.07 (d, J = 8.53 Hz, 2H), 4.46 (br s, 2H), 3.91 (t, J = 5.27 Hz, 2H), 3.30 (s, 3H), 2.70 (br s, 2H).

*2-(4-(2-Hydroxypropan-2-yl)phenyl)-7,8-dihydro-3H-pyrano[4,3-d]pyrimidin-4(5H)-one (**18**).* MeMgBr (3 M in Et2O, 780 μL, 2.34 mmol) was added to a ca. −78 °C mixture of compound **16** (0.99 mg, 0.346 mmol) in THF (3 mL). After complete addition, the reaction mixture was removed from the cold bath, stirred, and allowed to warm to room temperature over 1 h. The reaction mixture was cooled in an ice bath and slowly quenched with 1 N HCl (ca. 5 mL). The reaction mixture was then diluted with water and extracted with EtOAc (5 × 10 mL). The combined organic layers were dried over $MgSO_4$, filtered, and concentrated in vacuo to dryness, affording the title compound as an off-white solid (83 mg, 84% yield). Mass calculated for $C_{16}H_{18}N_2O_3$ 286.33, found 287.2 (ESI, M + H). 1H NMR (400 MHz, DMSO-d_6) δ ppm 12.63 (br s, 1H), 8.02 (d, J = 8.59 Hz, 2H), 7.59 (d, J = 8.59 Hz, 2H), 5.13 (s, 1H), 4.43 (s, 2H), 3.89 (t, J = 5.56 Hz, 2H), 2.66 (t, J = 5.05 Hz, 2H), 1.45 (s, 6H).

*2-Chloromethyl-3,5,7,8-tetrahydropyrano[4,3-d]pyrimidin-4-one (**45**).* A mixture of 4-oxo-tetrahydropyran-3-carboxylic acid methyl ester (1780 g, 11 mol) and NEt_3 (830 g, 8.2 mol) in MeOH (3560 mL) was cooled to 0 °C under N_2. A solution of 2-chloroacetamidine (567 g, 4.4 mol) in 890 mL of MeOH was added dropwise over 50 min. The reaction mixture was stirred at 0 °C for 30 min and then at about 20 °C for 16 h. LCMS at 215 nm and TLC (DCM:MeOH = 10:1) analysis showed that most of 4-oxotetrahydropyran-3-carboxylic acid methyl ester was consumed. The mixture was then filtered and concentrated to give a black oil, which was subsequently purified by flash column chromatography on silica gel and eluted with DCM to give a yellow solid/oil mixture, which was further triturated with MTBE (~1200 mL) and H_2O:CH_3CN:EA = 1:1:2 (~600 mL) to give the title compound as a white solid (318 g, 1.59 mol, 36% yield). MS m/z 201.2 (M + H). CHN analysis: calculated (results). C 47.89 (47.95), H 4.52 (4.401), N 13.96 (13.76).

*2-(Azidomethyl)-7,8-dihydro-3H-pyrano[4,3-d]pyrimidin-4(5H)-one (**46**).* To a solution of **45** (20.6 g, 103 mmol) in acetone (513 mL) was added an aqueous solution of sodium azide (7.01 g, 108 mmol in 32 mL of water). The reaction was stirred at room temperature for 36 h. Mixture was split into three equal volumes and each was diluted with dichloromethane (500 mL) and brine was added (100 mL) and the layers were separated. The aqueous fractions were combined and extracted with dichloromethane (5 × 100 mL). The combined organic layers were concentrated in vacuo. The resulting residue was taken up in dichloromethane (200 mL) and evaporated to dryness three times to yield 19.25 g (92 mmol, 90% yield) of a yellow-white solid. ^{1}H NMR (400 MHz, DMSO-d_6): δ 12.58 (br s, 1H), 4.36 (s, 2H), 4.28 (s, 2H), 3.85 (t, J = 5.56 Hz, 2H), 2.59 (t, J = 5.56 Hz, 2H).

*2-(Aminomethyl)-7,8-dihydro-3H-pyrano[4,3-d]pyrimidin-4(5H)-one (**47**).* To a solution of 2-(azidomethyl)-7,8-dihydro-3*H*-pyrano-[4,3-*d*]pyrimidin-4(5*H*)-one (19 g, 92 mmol) in THF (945 mL) at 35 °C was added triphenylphosphine (26.5 g, 101 mmol). Gas evolution was noted immediately and after approximately 40 min a fine precipitate formed. The reaction was allowed to stir for 1.5 h then 18.17 mL water was added. After an addition 2 h the reaction mixture was cooled to room temperature, filtered twice, concentrated to approximately 1/3 of the original volume and filtered once more. The solid material was washed with THF to yield a total of 15.82 g (87 mmol, 95% yield) of the title compound. ^{1}H NMR (400 MHz, MeOD): δ 4.49 (s, 2H), 3.94 (t, J = 5.56 Hz, 2H), 3.76 (s, 2H), 2.66 (t, J = 5.56 Hz, 2H).

*N-((4-Oxo-3,4-dihydroquinazolin-2-yl)methyl)-3-phenyl-N-(thiophen-2-ylmethyl)propanamide (**19**).* To a solution of 2-(((thiophen-2-ylmethyl)amino)methyl)quinazolin-4(3*H*)-one (100 mg, 0.369 mmol) in methylene chloride (4 mL) were added triethylamine (113 μL, 0.811 mmol, 2.2 equiv) and 3-phenylpropanoyl chloride (75 mg, 0.442 mmol, 1.2 equiv), and the solution was stirred 4 h. The reaction mixture was concentrated in vacuo, taken up in EtOAc, washed with brine, dried over Na_2SO_4, and concentrated in vacuo to give a white solid. The crude product was absorbed onto silica gel and added to an Analogix SF15-12g column, and compound was eluted with 1% to 10% MeOH in DCM over 12 column volumes on a Biotage SP1. This product was absorbed onto silica gel and added to an Biotage SNAP-10g column, and the compound was eluted with 5% to 80% EtOAc in dichloromethane over 12 column volumes on a Biotage SP1. The concentrated fractions were recrystallized from diethyl ether, washed with hepatne, and dried under vacuum to give the title compound (30 mg, 0.074 mmol, 20% yield). Mass calculated for $C_{23}H_{21}N_3O_2S$ 403.1, found 404.3 (ESI, M + H). ^{1}H NMR (400 MHz, chloroform-*d*) δ 10.13 (br s, 1H), 8.28 (d, J = 7.58 Hz, 1H), 7.71−7.78 (m, 1H), 7.64 (d, J = 8.08 Hz, 1H), 7.45−7.53 (m, 1H), 7.14−7.25 (m, 6H), 6.88−6.95 (m, 2H), 4.66 (s, 2H), 4.51 (s, 2H), 3.03−3.10 (m, 2H), 2.80−2.87 (m, 2H).

*General Procedure C. 2-(((Thiophen-2-ylmethyl)amino)methyl)-7,8-dihydro-3H-pyrano[4,3-d]pyrimidin-4(5H)-one (**23**).* A mixture of thiophene-2-carbaldehyde (0.021 mL, 0.22 mmol), **47** (40 mg, 0.22 mmol), and siliabond cyanoborohydride (240 mg, 0.24 mmol, 1 mmol/g) in ethanol (1 mL) was stirred at ambient temperature for 10 min. Acetic acid (0.013 mL, 0.22 mmol) was then added, and the mixture was stirred at ambient temperature for another 5 min. The reaction mixture was concentrated in vacuo and purified via flash column chromatography (ethyl acetate/hexane, 10:90 to 100:0, then

dx.doi.org/10.1021/jm400807n | J. Med. Chem. XXXX, XXX, XXX−XXX

methanol/dichloromethane, 1:99 to 10:90) to provide the title compound (30 mg, 49% yield). *m/z* 278.1 (M + H), retention time = 0.89 min. ^{1}H NMR (400 MHz, MeOD): δ 7.58 (d, J = 5.05 Hz, 1H), 7.33 (d, J = 3.03 Hz, 1H), 7.07−7.16 (m, 1H), 4.63 (s, 2H), 4.47 (s, 2H), 4.24 (s, 2H), 3.94 (t, J = 5.56 Hz, 2H), 2.73 (t, J = 5.56 Hz, 2H).

*General Procedure D. N-((4-Oxo-4,5,7,8-tetrahydro-3H-pyrano-[4,3-d]pyrimidin-2-yl)methyl)-3-phenyl-N-(thiophen-2-ylmethyl)-propanamide (**20**).* To a solution of compound **23** (95 mg, 0.34 mmol) in methylene chloride (3 mL) were added triethylamine (143 μL, 1.028 mmol) and 3-phenylpropanoyl chloride (58 mg, 0.34 mmol), and the solution was stirred 4 h. Purification was accomplished on an Isco 12 g column with 1% to 10% methanol in methylene chloride over 12 column volumes. The resulting partial purified product was taken up in DMSO and purified on a Sunfire C18 5 μm (19 × 100 mm) column. The mobile phase was 10% to 90% acetonitrile in water (0.1% TFA) to give title compound (39 mg, 0.095 mmol, 28% yield). Mass calculated for $C_{22}H_{23}N_3O_3S$ 409.5, found 410.6 (ESI, M + H); ^{1}H NMR (400 MHz, MeOD) δ ppm 7.09−7.39 (m, 5H), 6.79−7.00 (m, 2H), 4.77 (s, 1H), 4.35−4.49 (m, 4H), 3.79−3.98 (m, 2H), 3.35 (s, 1H), 2.81−3.01 (m, 3H), 2.73 (t, J = 7.33 Hz, 1H), 2.49−2.68 (m, 2H).

*2-((Ethylamino)methyl)-7,8-dihydro-3H-pyrano[4,3-d]pyrimidin-4(5H)-one (**21a**).* The title compound (20 mg, 35% yield) was prepared using general procedure C from acetaldehyde (0.015 mL, 0.28 mmol) and **47** (50 mg, 0.28 mmol). Mass calculated for $C_{10}H_{15}N_3O_2$ 209.2, found 210.3 (ESI, M + H). ^{1}H NMR (400 MHz, CD_3OD) δ 4.49 (s, 2H) 3.94 (t, J = 5.52 Hz, 2H) 3.79 (s, 2H) 2.85 (q, J = 7.36 Hz, 2H) 2.65 (t, J = 5.52 Hz, 2H) 1.22 (t, J = 7.28 Hz, 3H).

*N-Ethyl-N-((4-oxo-4,5,7,8-tetrahydro-3H-pyrano[4,3-d]pyrimidin-2-yl)methyl)-3-phenylpropanamide (**21**).* The title compound (11 mg, 4% yield) was prepared using general procedure D from **21a** (20 mg, 0.096 mmol) and 3-phenylpropanoyl chloride (14 μL, 0.096 mmol). HRMS calculated for $C_{19}H_{23}N_3O_3$ 342.1818, found (ESI, [M + H]$^+$), 342.1811. ^{1}H NMR (400 MHz, $CDCl_3$): δ 6.55−6.78 (m, 5H), 4.02 (s, 2H), 3.82 (s, 2H), 3.40 (t, J = 5.3 Hz, 2H), 2.82 (q, J = 6.5 Hz, 2H), 2.37−2.56 (m, 2H), 2.01−2.22 (m, 4H), 0.71 (s, 1H), 0.45−0.64 (m, 3H).

*N-((4-Oxo-4,5,7,8-tetrahydro-3H-pyrano[4,3-d]pyrimidin-2-yl)-methyl)-3-phenylpropanamide (**22**).* To a solution of **47** (24 mg, 0.130 mmol) in dichloromethane (1 mL) were added triethylamine (0.054 mL, 0.39 mmol, 3.0 equiv) and 3-phenylpropanoyl chloride (0.02 mL, 0.130 mmol, 1.0 equiv). The mixture was stirred at room temperature overnight. The solvent was removed, silica gel was added with methanol, and the mixture was concentrated in vacuo. The residue was purified using flash column chromatography (10g Isco column, 0 to 10% methanol/methylene chloride) to give the title compound (25 mg, 0.077 mmol, 59% yield). Mass calculated for $C_{17}H_{19}N_3O_3$ 313.1, found 314.3 (ESI, M + H). ^{1}H NMR (400 MHz, MeOH-d_4) δ 7.12−7.26 (m, 5H), 4.47 (s, 2H), 4.22 (s, 2H), 3.93 (t, J = 5.56 Hz, 2H), 2.87−2.96 (m, 2H), 2.62−2.67 (m, 2H), 2.54−2.61 (m, 2H).

*N-((4-Oxo-4,5,7,8-tetrahydro-3H-pyrano[4,3-d]pyrimidin-2-yl)-methyl)-3-phenyl-N-(thiophen-3-ylmethyl)propanamide (**24**).* Following the general procedure D, the title compound was prepared. Mass calculated for $C_{22}H_{23}N_3O_3S$ 409.5, found 410.6 (ESI, M + H). ^{1}H NMR (MeOD) δ ppm 7.43 (dd, J = 5.05, 3.03 Hz, 1H), 7.11−7.39 (m, 6H), 6.88−7.02 (m, 1H), 4.74 (s, 1H), 4.67 (s, 1H), 4.44 −4.56 (m, 3H), 4.41 (s, 1H), 3.95 (q, J = 5.56 Hz, 2H), 2.95−3.09 (m, 2 H), 2.77−2.95 (m, 2 H), 2.58−2.74 (m, 2 H).

*N-((4-Oxo-4,5,7,8-tetrahydro-3H-pyrano[4,3-d]pyrimidin-2-yl)-methyl)-3-(pyridin-4-yl)-N-(thiophen-2-ylmethyl)propanamide (**25**).* To a solution of **23** (100 mg, 0.369 mmol, 1.0 equiv) and 3-(pyridin-4-yl)propanoic acid (26 mg, 0.173 mmol, 1.0 equiv) in methylene chloride (1 mL) were added triethylamine (51 μL, 0.346 mmol, 2.0 equiv) and 2-chloro-1,3-dimethylimidazolidinium chloride (35 mg, 0.2 mmol, 1.2 equiv), and the solution was stirred overnight at room temperature. The reaction mixture was diluted with dichloromethane, washed with water (2×), dried over Na_2SO_4, and concentrated in vacuo. The residue was dissolved in 1 mL of DMSO and purified on a Xterra C8 5 μm (19 × 100 mm) column, eluting with 10% to 70% MeCN in water (0.1% TFA) over 15 min. The fractions were combined and concentrated in vacuo. The product was dissolved MeOH, added to a SCX column (1 g), and washed with MeOH (100 mL), and then the product was eluted with 1 N NH_3 in MeOH (50 mL) and concentrated to provide the title compound (15 mg, 0.034 mmol, 23% yield). HRMS calculated for $C_{21}H_{22}N_4O_3S$ 411.1491 (M + H), found 411.1507 (ESI, [M + H]$^+$). ^{1}H NMR (400 MHz, methanol-d_4) δ 8.73 (d, J = 5.56 Hz, 2H), 7.96−8.12 (m, 2H), 7.20−7.45 (m, 1H), 6.77−7.16 (m, 2H), 4.95−5.14 (m, 2H), 4.56−4.81 (m, 4H), 3.91−4.19 (m, 3H), 3.34 (d, J = 6.06 Hz, 1H), 2.78−3.28 (m, 4H).

*N-((4-Oxo-4,5,7,8-tetrahydro-3H-pyrano[4,3-d]pyrimidin-2-yl)-methyl)-3-(pyridin-3-yl)-N-(thiophen-2-ylmethyl)propanamide (**26**).* The title compound (10 mg, 0.022 mmol, 15% yield) was prepared following the same procedure as that for compound **25** from **23** (40 mg, 0.144 mmol, 1.0 equiv) and 3-(pyridin-3-yl)propanoic acid (26 mg, 0.173 mmol, 1.0 equiv). HRMS calculated for $C_{21}H_{22}N_4O_3S$ 411.1491 (M + H), found 411.1492 (ESI, [M + H]$^+$). 1H NMR (400 MHz, methanol-d_4) δ 8.54−8.92 (m, 3H), 7.98−8.07 (m, 1H), 7.20−7.44 (m, 1H), 6.76−7.13 (m, 2H), 4.93−5.11 (m, 1H), 4.49−4.79 (m, 5H), 3.95−4.15 (m, 3H), 2.76−3.28 (m, 6H).

*3-(2-Fluorophenyl)-N-((4-oxo-4,5,7,8-tetrahydro-3H-pyrano[4,3-d]pyrimidin-2-yl)methyl)-N-(thiophen-2-ylmethyl)propanamide (**27**).* To a solution of **47** (45 mg, 0.16 mmol) and 3-(2-fluorophenyl)propionic acid (27 mg, 0.16 mmol) in dichloromethane (1 mL) were added 1-(3-dimethylaminopropyl)-3-ethylcarbodiimide hydrochloride (37 mg, 0.20 mmol), 1-hydroxybenzotriazole (25 mg, 0.16 mmol), and triethylamine (68 μL, 0.49 mmol). The mixture was stirred at ambient temperature for 24 h. The mixture was added water and then extracted with dichloromethane two times. The combined organic layer was concentrated in vacuo and purified via flash column chromatography (ethyl acetate:hexane, 10:90 to 100:0) to give a residue. The residue was further purified via HPLC to provide the title compound (12 mg, 17% yield). HRMS calculated for $C_{22}H_{22}FN_3O_3S$ 428.1444, found (ESI, [M + H]$^+$), 428.1439. ^{1}H NMR (400 MHz, $CDCl_3$) δ 10.49 (br s, 1H), 7.15−7.34 (m, 3H), 6.86−7.15 (m, 4H), 4.72 (s, 2H), 4.58 (s, 2H), 4.38−4.48 (m, 2H), 3.95 (t, J = 5.5 Hz, 2H), 3.09 (t, J = 7.8 Hz, 2H), 2.86 (t, J = 7.5 Hz, 2H), 2.57−2.72 (m, 2H).

*3-(3-Fluorophenyl)-N-((4-oxo-4,5,7,8-tetrahydro-3H-pyrano[4,3-d]pyrimidin-2-yl)methyl)-N-(thiophen-2-ylmethyl)propanamide (**28**).* The title compound (8 mg, 11% yield) was prepared according to same procedure as that for compound **27** from 3-(3-fluorophenyl)-propanoic acid. HRMS calculated for $C_{22}H_{22}FN_3O_3S$ 428.1444, found (ESI, [M + H]$^+$), 428.1454. ^{1}H NMR (400 MHz, $CDCl_3$) δ 10.66 (br s, 1H), 7.20−7.38 (m, 2H), 6.84−7.07 (m, 5H), 4.72 (s, 2H), 4.57 (s, 2H), 4.44 (s, 2H), 3.95 (t, J = 5.5 Hz, 2H), 3.05 (t, J = 7.5 Hz, 2H), 2.85 (t, J = 7.5 Hz, 2H), 2.54−2.76 (m, 2H).

*3-(4-Fluorophenyl)-N-((4-oxo-4,5,7,8-tetrahydro-3H-pyrano[4,3-d]pyrimidin-2-yl)methyl)-N-(thiophen-2-ylmethyl)propanamide (**29**).* The title compound (20 mg, 43% yield) was prepared according to same procedure as that for compound **27** from 2-((thiophen-2-ylmethylamino)methyl)-7,8-dihydro-3*H*-pyrano[4,3-*d*]pyrimidin-4(5*H*)-one (30 mg, 0.11 mmol) and 3-(4-fluorophenyl)propanoic acid (18 mg, 0.11 mmol). HRMS calculated for $C_{22}H_{22}FN_3O_3S$ 428.1444, found (ESI, [M + H]$^+$), 428.1454. ^{1}H NMR (400 MHz, $CDCl_3$) δ 10.55 (br s 1H), 7.23−7.33 (m, 1H), 7.11−7.22 (m, 2H), 6.92−7.05 (m, 3H), 6.88 (d, J = 3.0 Hz, 1H), 4.70 (s, 2H), 4.58 (s, 2H), 4.42 (s, 2H), 3.95 (t, J = 5.5 Hz, 2H), 3.03 (t, J = 7.3 Hz, 2H), 2.82 (t, J = 7.5 Hz, 2H), 2.65 (t, J = 5.5 Hz, 2H).

*3-(2-Hydroxyphenyl)-N-((4-oxo-4,5,7,8-tetrahydro-3H-pyrano-[4,3-d]pyrimidin-2-yl)methyl)-N-(thiophen-2-ylmethyl)-propanamide (**30**).* The title compound (6 mg, 8% yield) was prepared according to same procedure as that for compound **27** from 3-(2-hydroxyphenyl)propionic acid. HRMS calculated for $C_{22}H_{23}N_3O_4S$ 426.1488, found (ESI, [M + H]$^+$), 426.1481. ^{1}H NMR (400 MHz, $CDCl_3$) δ 10.91 (br s, 1H), 8.21 (br s, 1H), 7.08−7.33 (m, 1H), 6.93−7.08 (m, 2H), 6.63−6.93 (m, 4H), 4.54 (s, 2H), 4.48 (s, 2H), 4.37 (s, 2H), 3.86 (t, J = 5.5 Hz, 2H), 2.94−3.07 (m, 2H), 2.78−2.94 (m, 2H), 2.52−2.63 (m, 2H).

3-(3-Hydroxyphenyl)-N-((4-oxo-4,5,7,8-tetrahydro-3H-pyrano-[4,3-d]pyrimidin-2-yl)methyl)-N-(thiophen-2-ylmethyl)-

dx.doi.org/10.1021/jm400807n | J. Med. Chem. XXXX, XXX, XXX−XXX

*propanamide (**31**).* The title compound (7 mg, 10% yield) was prepared according to same procedure as that for compound **27** from 3-(3-hydroxyphenyl)propionic acid. HRMS calculated for $C_{22}H_{23}N_3O_4S$ 426.1488, found (ESI, $[M + H]^+$), 426.1494. ^1H NMR (400 MHz, $CDCl_3$) δ 10.78 (br s, 1H), 7.23 (d, J = 5.0 Hz, 1H), 7.17 (t, J = 7.8 Hz, 1H), 7.10 (br s, 1H), 6.86−6.98 (m, 1H), 6.74 (t, J = 6.8 Hz, 4H), 4.56 (d, J = 18.1 Hz, 4H), 4.46 (s, 2H), 3.94 (t, J = 5.5 Hz, 2H), 2.96−3.15 (m, 2H), 2.79−2.91 (m, 2H), 2.63 (t, J = 5.5 Hz, 2H).

*3-(4-Hydroxyphenyl)-N-((4-oxo-4,5,7,8-tetrahydro-3H-pyrano-[4,3-d]pyrimidin-2-yl)methyl)-N-(thiophen-2-ylmethyl)-propanamide (**32**).* The title compound (7 mg, 9% yield) was prepared according to same procedure as that for compound **27** from 3-(4-hydroxyphenyl)propionic acid. HRMS calculated for $C_{22}H_{23}N_3O_4S$ 426.1488, found (ESI, $[M + H]^+$), 426.1493. ^1H NMR (400 MHz, $CDCl_3$): δ 11.17 (br s, 1H), 7.27−7.29 (m, 1H), 7.04 (m, J = 7.5 Hz, 2H), 6.93−7.00 (m, 1H), 6.89 (d, J = 3.0 Hz, 1H), 6.72 (m, J = 8.0 Hz, 2H), 4.71 (br s, 2H), 4.54 (br s, 2H), 4.44 (s, 2H), 3.95 (t, J = 5.3 Hz, 2H), 2.97 (t, J = 7.0 Hz, 2H), 2.83 (t, J = 7.0 Hz, 2H), 2.67 (br s, 2H).

*Ethyl 2-(4-(4-Fluorobenzoyl)piperidin-1-yl)acetate (**48**).* To a solution of (4-fluorophenyl)(piperidin-4-yl)methanone hydrochloride (51.8 g, 213 mmol) in acetonitrile (400 mL) were added ethyl 2-bromoacetate (38.2 mL, 345 mmol) and triethylamine (70 mL, 506 mmol). The mixture was heated at reflux for 5 h. The solvent was evaporated under reduced pressure and purified via flash column chromatography (ethyl acetate/hexane, 10:90 to 100:0) to provide the title compound (52.7 g, 85% yield). MS m/z 294.4 (M + 1), retention time = 1.94 min. ^1H NMR (400 MHz, $CDCl_3$) δ 7.98 (dd, J = 8.5, 5.5 Hz, 2 H), 7.16 (t, J = 8.5 Hz, 2 H), 4.22 (q, J = 7.2 Hz, 2 H), 3.16−3.27 (m, 1 H), 3.03 (d, J = 11.5 Hz, 2 H), 2.43 (td, J = 11.2, 3.3 Hz, 2 H), 1.81−2.09 (m, 4 H), 1.51−1.73 (m, 2 H), 1.30 (t, J = 7.3 Hz, 3 H).

*2-(4-(4-Fluorobenzoyl)piperidin-1-yl)acetic Acid (**50**).* To a solution of **48** (52.7 g, 180 mmol) in ethanol (300 mL) was added sodium hydroxide solution in water (1.8 M, 300 mL). The mixture was stirred at ambient temperature for 24 h and then neutralized with HCl (37%) until pH 5−7. The solvent was evaporated under reduced pressure, dissolved with methanol and methylene chloride, and filtered. The resulting solution was evaporated to give the title compound as a white solid (47.7 g, >99% yield). MS m/z 266.3 (M + H), retention time = 0.87 min. ^1H NMR (400 MHz, CD_3OD) δ 8.11 (dd, J = 8.8, 5.3 Hz, 2H), 7.26 (t, J = 8.8 Hz, 2H), 3.57−3.85 (m, 5H), 3.21 (t, J = 11.0 Hz, 2H), 1.96−2.18 (m, 4H).

*2-(4-(4-Fluorobenzoyl)piperidin-1-yl)-N-((4-oxo-4,5,7,8-tetrahydro-3H-pyrano[4,3-d]pyrimidin-2-yl)methyl)acetamide (**34**).* To a solution of **47** (1.7 g, 9.6 mmol) and **50** (2.7 g, 10 mmol) in dichloromethane (50 mL) were added 1-(3-dimethylaminopropyl)-3-ethylcarbodiimide hydrochloride (2.2 g, 11 mmol), 1-hydroxybenzotriazole (1.5 g, 9.6 mmol), and triethylamine (4.0 mL, 29 mmol). The mixture was stirred at ambient temperature for 24 h. The reaction mixture was washed with ammonium chloride solution, concentrated in vacuo, and purified via flash column chromatography (ethyl acetate/hexane, 10:90 to 100:0, then methanol/dichloromethane, 1:99 to 10:90) to provide the title compound (2.2 g, 54% yield). HRMS calculated for $C_{22}H_{25}N_4O_4$ 429.1938, found (ESI, $[M + H]^+$), 429.1925. MS m/z 429.3 (M + 1), retention time = 1.28 min. ^1H NMR (400 MHz, $CDCl_3$) δ 11.12 (s, 1H), 8.07 (s, 1H), 7.99 (dd, J = 9.0, 5.5 Hz, 2H), 7.18 (t, J = 8.5 Hz, 2H), 4.58 (s, 2H), 4.41 (d, J = 6.0 Hz, 2H), 3.97 (t, J = 5.5 Hz, 2H), 3.28 (m, 1H), 3.17 (m, 2H), 3.10 (m, 2H), 2.71 (m, 2H), 2.39 (m, 2H), 1.89 (m, 4H).

*2-(4-(4-Fluorobenzoyl)piperidin-1-yl)-N-((4-oxo-4,5,7,8-tetrahydro-3H-pyrano[4,3-d]pyrimidin-2-yl)methyl)-N-(thiophen-2-ylmethyl)acetamide (**35**).* The title compound (296 mg, 0.56 mmol, 25% yield) was prepared similar to that for compound **34** from 2-((thiophen-2-ylmethylamino)methyl)-7,8-dihydro-3*H*-pyrano[4,3-*d*]-pyrimidin-4(5*H*)-one (710 mg, 2.3 mmol) and **50** (720 mg, 2.7 mmol). HRMS calculated for $C_{27}H_{29}FN_4O_4S$ 525.1972, found (ESI, $[M + H]^+$), 525.1968. MS m/z 525.2 (M + 1), retention time = 3.08 min. ^1H NMR (400 MHz, DMSO-d_6) δ 11.93 (s, 1H), 8.00 (d, J = 8.8, 575 Hz, 2H), 7.38 (d, J = 4.4 Hz, 1H), 7.28 (t, J = 8.8 Hz, 2H), 7.00 (s, 1H), 6.95 (s, 1H), 4.85 (s, 2H), 4.47 (s, 2H), 4.38 (s, 2H), 3.85 (t, J = 5.7 Hz, 2H), 3.29 (m, 2H), 2.90 (m, 3H), 2.53 (t, J = 5.4 Hz, 2H), 2.29 (t, J = 10.7 Hz, 2H), 1.76 (m, 2H), 1.63 (m, 2H).

*2-((Benzylamino)methyl)-7,8-dihydro-3H-pyrano[4,3-d]-pyrimidin-4(5H)-one (**36a**).* Following general procedure E, the title compound (30 mg, 0.11 mmol, 11% yield) was prepared from phenylmethanamine (107 mg, 0.996 mmol). Mass calculated for $C_{15}H_{17}N_3O_2$ 271.3, found 272.4 (ESI, M + H).

*N-Benzyl-2-(4-(4-fluorobenzoyl)piperidin-1-yl)-N-((4-oxo-4,5,7,8-tetrahydro-3H-pyrano[4,3-d]pyrimidin-2-yl)methyl)acetamide (**36**).* Following the procedure for compound **34**, the title compound (17.7 mg, 0.034 mmol, 18% yield) was prepared from **36a** (46 mg, 0.170 mmol) and **50** (50 mg, 0.19 mmol). Mass calculated for $C_{29}H_{31}FN_4O_4$ 518.6, found 519.4 (ESI, M + H). ^1H NMR (400 MHz, dichloromethane-d_2) δ 7.98 (br s, 2H) 7.28−7.52 (m, 1H) 7.21 (d, J = 7.58 Hz, 4H) 4.66 (d, J = 8.08 Hz, 2H) 4.60 (br s, 1H) 4.48 (br s, 2H) 3.85−4.08 (m, 5H) 3.81 (br s, 2H) 3.42 (d, J = 7.07 Hz, 2H) 3.28 (br s, 2H) 2.70 (d, J = 15.66 Hz, 2H) 2.06−2.36 (m, 3H) 1.17−1.41 (m, 2H).

*2-(((Pyridin-2-ylmethyl)amino)methyl)-7,8-dihydro-3H-pyrano-[4,3-d]pyrimidin-4(5H)-one (**37a**).* A mixture of **47** (150 mg, 0.83 mmol) and 2-(bromomethyl)pyridine (168 mg, 0.66 mmol) was heated via microwave in ethanol (1.5 mL) at 120 °C for 5 min. The reaction mixture was concentrated in vacuo, and the residue was purified via flash column chromatography (ethyl acetate/hexane, 20:80 to 100:0 and then methanol/dichloromethane, 1:99 to 30:70) to provide the title compound (225 mg, 100% yield). MS m/z 273.2 (M + 1), retention time = 0.78 min.

*2-(4-(4-Fluorobenzoyl)piperidin-1-yl)-N-((4-oxo-4,5,7,8-tetrahydro-3H-pyrano[4,3-d]pyrimidin-2-yl)methyl)-N-(pyridin-2-ylmethyl)-acetamide (**37**).* Following the procedure for compound **34**, the title compound (20 mg, 0.038 mmol, 8% yield) was prepared from **37a** (130 mg, 0.477 mmol) and **50** (149 mg, 0.477 mmol). HRMS calculated for $C_{28}H_{30}FN_5O_5$ 520.2360, found (ESI, $[M + H]^+$), 520.2367. Retention time = 4.44 min. ^1H NMR (400 MHz, $CDCl_3$) δ 16.14 (br s, 0.5H), 14.65 (br s, 0.5H), 8.81−8.97 (m, 1H), 7.99−8.08 (m, 2H), 7.82−7.98 (m, 1H), 7.46−7.53 (m, 1H), 7.35−7.43 (m, 1H), 7.19−7.29 (m, 2H), 5.20 (s, 1H), 4.84 (s, 2H), 4.69 (s, 1H), 4.58 (s, 1H), 4.02−4.23 (m, 2H), 3.15−3.28 (m, 2H), 2.86−2.97 (m, 2H), 2.75−2.85 (m, 2H), 2.17−2.40 (m, 2H), 1.85 (d, J = 10.54 Hz, 4H), 1.54−1.73 (m, 2H).

*General Procedure E. 2-((Isobutylamino)methyl)-7,8-dihydro-3H-pyrano[4,3-d]pyrimidin-4(5H)-one (**38a**).* To a solution of **45** (50 mg, 0.25 mmol) in 3 mL of EtOH was added 2-methylpropan-1-amine (40 mg, 0.54 mmol, 2.2 equiv). The resulting mixture was heated at 65 °C overnight. After 18 h, the reaction mixture was concentrated in vacuo to give an oil that was dissolved in MeOH and added to a SCX column. The SCX column was washed with MeOH, and the product was eluted with 1 N NH_3 in MeOH and concentrated in vacuo. The crude product was absorbed onto silica gel and added to an Biotage SNAP-10g column, and compound was eluted with 1% to 10% MeOH in dichloromethane over 12 column volumes to provide the title compound (13.7 mg, 0.058 mmol, 23% yield). Mass calculated for $C_{12}H_{19}N_3O_2$ 237.30, found 238.4 (ESI, M + H).

*2-(4-(4-Fluorobenzoyl)piperidin-1-yl)-N-isobutyl-N-((4-oxo-4,5,7,8-tetrahydro-3H-pyrano[4,3-d]pyrimidin-2-yl)methyl)-acetamide (**38**).* To a solution of **50** (50 mg, 0.188 mmol) and diisopropylethylamine (0.082 mL, 0.47 mmol) in DMF (1 mL) was added HATU (107 mg, 0.283 mmol, 1.5 equiv), and the mixture was stirred for 30 min. Then **38a** (40 mg, 0.170 mmol) in DMP (1 mL) was added, and mixture was stirred at ambient temperature overnight. The crude reaction was purified directly by prep-HPLC on a Sunfire C18−5 μm (19 × 100 mm) column, eluting with 10% to 90% MeCN in water (0.1% TFA) over 10 min to provide the title compound (36.4 mg, 0.058 mmol, 31% yield). Exact mass calculated for $C_{26}H_{33}FN_4O_4$ 485.2564, found 485.2588 (ESI, M + H). ^1H NMR (400 MHz, dichloromethane-d_2) δ ppm 7.98 (dd, J = 8.84, 5.31 Hz, 2H), 7.20 (t, J = 8.59 Hz, 2H), 4.48−4.67 (m, 4H), 4.21 (br s, 2H), 3.89−4.01 (m, 2H), 3.82 (br s, 3H), 3.23 (br s, 4H), 2.62−2.83 (m, 2H), 2.19 (br s,

dx.doi.org/10.1021/jm400807n | J. Med. Chem. XXXX, XXX, XXX−XXX

3H), 2.13 (s, 1H), 2.07 (d, J = 6.57 Hz, 1H), 0.98 (d, J = 6.57 Hz, 4H), 0.88 (d, J = 5.56 Hz, 2H).

*2-((Propylamino)methyl)-7,8-dihydro-3H-pyrano[4,3-d]-pyrimidin-4(5H)-one (**39a**).* Following general procedure E, the title compound (41 mg, 0.173 mmol, 69% yield) was prepared from **45** (50 mg, 0.25 mmol) and propylamine (59 mg, 0.997 mmol). Mass calculated for $C_{11}H_{17}N_3O_2$ 223.2, found 224.3 (ESI, M + H).

*2-(4-(4-Fluorobenzoyl)piperidin-1-yl)-N-((4-oxo-4,5,7,8-tetrahydro-3H-pyrano[4,3-d]pyrimidin-2-yl)methyl)-N-propylacetamide (**39**).* Following the procedure for compound **38**, the title compound (37.3 mg, 0.064 mmol, 34% yield) was prepared from **39a** (38 mg, 0.170 mmol) and **50** (50 mg, 0.188 mmol). Exact mass calculated for $C_{25}H_{31}FN_4O_4$ 471.2408, found 471.2400 (ESI, M + H). ^{1}H NMR (400 MHz, dichloromethane-d_2) δ ppm 7.89 (dd, J = 2.78, 5.81 Hz, 2H), 7.10 (t, J = 8.34 Hz, 2H), 4.37−4.56 (m, 4H), 4.19 (br s, 2H), 3.38−3.91 (m, 6H), 2.97−3.37 (m, 4H), 2.55−2.96 (m, 2H), 1.83−2.37 (m, 3H), 0.97−1.68 (m, 2H), 0.65−0.93 (m, 3H).

*N-Ethyl-2-(4-(4-fluorobenzoyl)piperidin-1-yl)-N-((4-oxo-4,5,7,8-tetrahydro-3H-pyrano[4,3-d]pyrimidin-2-yl)methyl)acetamide (**40**).* To a solution of **45** (100 mg, 0.498 mmol) in EtOH (2 mL) was added ethylamine (128 mg, 1.99 mmol, 70% in water). The mixture was then heated at 65 °C for 16 h and concentrated to give 2-((ethylamino)methyl)-7,8-dihydro-3H-pyrano[4,3-d]pyrimidin-4(5H)-one (**40a**) as a crude yellow solid. This solid (103 mg, 0.493 mmol) was reacted with **50** (131 mg, 0.493 mmol) and O-(7-azabenzotriazol-1-yl)-N,N,N',N'-tetramethyluronium hexafluorophosphate (281 mg, 0.740 mmol) in DMF (2.5 mL) using diisopropylethylamine (159 mg, 1.23 mmol). The resulting mixture was stirred at ambient temperature for 16 h, and the crude product was concentrated to dryness. The solid was partitioned between ethyl acetate and aqueous sodium bicarbonate, and the layers were separated. The organic layer was washed with brine and aqueous citric acid, dried (magnesium sulfate), and concentrated to give a crude oil that was purified by flash column chromatography (0−10% methanol in dichloromethane) to give the title compound as a yellow solid (34 mg, 0.074 mmol, 15% yield). MS m/z 457.4 (M + H), Ret time: 1.25 min; HRMS m/z (M + H) calculated for $C_{24}H_{29}N_4O_4F$: 457.2248, found: 457.2251. ^{1}H NMR (400 MHz, CD_3OD) δ 8.00−8.14 (m, 2H), 7.27 (dt, J = 1.76, 8.66 Hz, 2H), 4.40−4.55 (m, 4H), 4.35 (br s, 1.3 H), 4.27 (br s, 0.7H), 3.87−3.98 (m, 2H), 3.72 (br s, 3H), 3.43−3.55 (m, 3H), 3.15−3.27 (m, 1H), 2.55−2.70 (m, 2H), 1.91−2.21 (m, 4H), 1.24−1.32 (m, 2H), 1.12 (t, J = 7.03 Hz, 1H) [individual rotamers could not be assigned].

*2-((Methylamino)methyl)-7,8-dihydro-3H-pyrano[4,3-d]-pyrimidin-4(5H)-one (**41a**).* Following general procedure E, the title compound (30.7 mg, 0.157 mmol) was prepared from **45** (50 mg, 0.25 mmol) and 30% methanamine (57 mg, 0.548 mmol) in water. Mass calculated for $C_9H_{13}N_3O_2$ 195.2, found 196.3 (ESI, M + H).

*2-(4-(4-Fluorobenzoyl)piperidin-1-yl)-N-methyl-N-((4-oxo-4,5,7,8-tetrahydro-3H-pyrano[4,3-d]pyrimidin-2-yl)methyl)acetamide (**41**).* Following the procedure for compound **38**, the title compound (22.5 mg, 0.50 mmol, 26% yield) was prepared from **41a** (33 mg, 0.169 mmol) and **50** (50 mg, 0.188 mmol). Exact mass calculated for $C_{23}H_{27}FN_4O_4$ 443.2095, found 443.2099 (ESI, M + H). ^{1}H NMR (400 MHz, dichloromethane-d_2) δ ppm 7.95−8.01 (m, 2H), 7.14−7.20 (m, 2H), 4.23−4.56 (m, 4H), 3.89−3.95 (m, 2H), 3.05−3.56 (m, 5H), 2.89 (s, 2H), 2.58−2.69 (m, 2H), 2.45−2.57 (m, 2H), 2.14−2.29 (m, 1H), 1.85−2.03 (m, 2H), 1.46 (t, J = 7.58 Hz, 2H).

*2-((Cyclopropylmethylamino)methyl)-7,8-dihydro-3H-pyrano-[4,3-d]pyrimidin-4(5H)-one (**42a**).* To a solution of **45** (1 g, 5 mmol, 1 equiv) and DIEA (4.35 mL, 24.9 mmol, 5 equiv) in 7 mL of EtOH was added cyclopropylmethylamine (1.4 g, 20 mmol, 4 equiv). The resulting mixture was heated at 65 °C overnight. After 18 h, the reaction mixture was concentrated in vacuo to give an oil that was purified by silica gel column chromatography (100% CH_2Cl_2) to give the title compound as a white solid (0.23 g, 20%). Mass calculated for $C_{12}H_{18}N_3O_2$ 236.1; MS (ESI) m/z 236.9 (M + H)$^+$. Retention time: 0.56 min (5−95% CH_3CN/H_2O over 2 min with 0.1% formic acid, Inertsil 3 × 3 mm C-8-3 column with flow rate of 2 mL/min). ^{1}H NMR (400 MHz, chloroform-d) δ ppm 4.37−4.42 (m, 2H), 3.95 (s, 1H), 3.80−3.88 (m, 3H), 2.63−2.72 (m, 1H), 2.54−2.63 (m, 3H), 0.89−1.05 (m, 1H), 0.42−0.54 (m, 2H), 0.14−0.26 (m, 2H).

*N-(Cyclopropylmethyl)-2-(4-(4-fluorobenzoyl)piperidin-1-yl)-N-((4-oxo-4,5,7,8-tetrahydro-3H-pyrano[4,3-d]pyrimidin-2-yl)methyl)-acetamide (**42**).* Following the procedure for compound **38**, the title compound (14.4 mg, 0.030 mmol, 16% yield) was prepared from 2-((cyclopropylmethylamino)methyl)-7,8-dihydro-3H-pyrano[4,3-d]-pyrimidin-4(5H)-one (44 mg, 0.188 mmol) and **50** (50 mg, 0.188 mmol). Exact mass calculated for $C_{26}H_{31}FN_4O_4$ 483.2408, found 483.2416 (ESI, M + H). ^{1}H NMR (400 MHz, dichloromethane-d_2) δ ppm 7.98 (dd, J = 5.56, 8.59 Hz, 2H), 7.19 (t, J = 8.59 Hz, 2H), 4.42−4.75 (m, 5H), 4.12−4.31 (m, 2H), 3.86−3.98 (m, 2H), 3.36−3.76 (m, 2H), 3.06−3.33 (m, 2H), 2.56−2.76 (m, 2H), 2.22 (br s, 4H), 0.79−1.04 (m, 1H), 0.61 (d, J = 7.58 Hz, 2H), 0.35−0.54 (m, 1H), 0.12−0.33 (m, 3H).

*[4-(4-Methoxybenzoyl)piperidin-1-yl]acetic Acid Ethyl Ester (**49**).* To a solution of (4-methoxyphenyl)(piperidin-4-yl)methanone (20 g, 78 mmol, 1 equiv) in acetonitrile (313 mL) was added triethylamine (22 mL, 156 mmol, 2 equiv), followed by ethyl 2-bromoacetate (9.5 mL, 86 mmol, 1.1 equiv) dropwise. The resulting mixture was heated at 85 °C overnight. After 18 h, the reaction mixture was diluted with saturated $NaHCO_3$ (150 mL) and extracted with ethyl acetate (3 × 500 mL). The combined organic layers were washed with brine, dried over anhydrous Na_2SO_4, filtered, and concentrated in vacuo to give an oil. This oil was purified by silica gel column chromatography (10−20% acetone/heptane) to give the title compound as a white solid (11.7 g, 49% yield). Mass calculated for $C_{17}H_{24}N_1O_4$ 306.2. MS (ESI) m/z 306.4 (M + H)$^+$.

*[4-(4-Methoxybenzoyl)piperidin-1-yl]acetic Acid (**51**).* To a solution of **49** (11.7 g, 38 mmol, 1 equiv) in 154 mL of EtOH was added a solution of NaOH (3.07 g, 77 mmol, 2 equiv) in 154 mL of H_2O. The resulting mixture was stirred at room temperature overnight. After 18 h, the reaction mixture was concentrated and treated with 1 N HCl to pH 5. The resulting mixture was freeze-dried using a lyophilizer to remove H_2O. The resulting yellow solid was washed with dichloromethane/methanol, and NaCl was filtered off. The filtrate was concentrated to give the title compound as a white solid (11 g, 38 mmol). Mass calculated for $C_{15}H_{20}NO_4$ 278.1. MS (ESI) m/z 278.8 (M + H)$^+$.

*N-(Cyclopropylmethyl)-2-(4-(4-methoxybenzoyl)piperidin-1-yl)-N-((4-oxo-4,5,7,8-tetrahydro-3H-pyrano[4,3-d]pyrimidin-2-yl)-methyl)acetamide (**43**).* To a solution of **51** (0.071 g, 0.26 mmol, 1 equiv) and DIEA (0.089 mL, 0.51 mmol, 2 equiv) in 2 mL of DMF was added HATU (0.107 g, 0.281 mmol, 1.1 equiv). The resulting mixture was stirred at room temperature for 30 min. **42a** (0.06 g, 0.26 mmol, 1 equiv) in 1 mL of DMF was added, and the mixture was stirred at room temperature overnight. The reaction mixture was diluted with H_2O (10 mL) and extracted with dichloromethane (3 × 50 mL). The combined organic layers were concentrated in vacuo and purified by preparative HPLC (20−100% CH_3CN/H_2O over 10 min with 0.1% TFA on a Sunfire C18 OBD 50 × 50 mm column with flow rate of 60 mL/min) to give the title compound as a white solid (0.03 g, 0.06 mmol, 24% yield). HRMS calculated for $C_{27}H_{35}N_4O_5$ 495.2607, found (ESI, [M + H]$^+$) 495.2606. MS (ESI) m/z 495.3 (M + H)$^+$. Retention time: 2.89 min (5−95% CH_3CN/H_2O over 7.75 min with 0.1% formic acid, Inertsil ODS3 100 × 3 mm C18 column with flow rate of 1.0 mL/min). ^{1}H NMR (400 MHz, MeOD) δ ppm 12.20−12.62 (m, 1H), 7.88−7.97 (m, 2H), 7.03 (dd, J = 5.56, 8.59 Hz, 2H), 4.58 (s, 1H), 4.30−4.44 (m, 3H), 3.77−3.86 (m, 5H), 3.44 (d, J = 7.07 Hz, 1H), 3.32−3.39 (m, 1H), 3.13−3.27 (m, 4H), 2.76−3.00 (m, 2H), 2.44 (br s, 1H), 2.04−2.21 (m, 2H), 1.50−1.77 (m, 3H), 1.31−1.46 (m, 1H), 0.86−1.11 (m, 1H), 0.33−0.48 (m, 2H), 0.13−0.27 (m, 2H).

■ ASSOCIATED CONTENT

Supporting Information

Graphs of calculated versus measured log P as well as thermodynamic data. This material is available free of charge via the Internet at http://pubs.acs.org.

dx.doi.org/10.1021/jm400807n | J. Med. Chem. XXXX, XXX, XXX−XXX

Accession Codes

PDB codes for the TNKS1 structures in complex with **19**, **33**, and **35** are 4LI6, 4LI7, and 4LI8, respectively.

AUTHOR INFORMATION

Corresponding Author

*Phone: 617-871-7551. E-mail: michael.shultz@novartis.com.

Present Addresses

‡Blueprint Medicines, 215 First St., Cambridge, MA 02142.
§Chongqing Pharmaceutical Research Institute, No. 565, Tushan Rd., Nanan District, Chongqing, China 400061.
∥Anti-Infective Group, Medicinal Chemistry, Actelion Pharmaceuticals Ltd., Gewerbestrasse 16, CH-4123 Allschwil, Switzerland.
⊥Vertex Pharmaceuticals, Inc., 130 Waverly St., Cambridge, MA 02139.
#Sanofi-Oncology, 640 Memorial Dr., Cambridge, MA 02139.
□Epizyme, 400 Technology Square, Cambridge, MA 02139.

Notes

The authors declare no competing financial interest.

ACKNOWLEDGMENTS

The authors thank Tim Ramsey for many helpful suggestions during the preparation of this manuscript. We would like to acknowledge the work of James Groarke and Guoping Xiao for protein purification of TNKS1. The TNKS1/33 data collection was performed on the 5.0.3 beamline at the Advanced Light Source at Berkeley Lab. The Berkeley Center for Structural Biology is supported in part by the National Institutes of Health, National Institute of General Medical Sciences, and the Howard Hughes Medical Institute. The Advanced Light Source is supported by the Director, Office of Science, Office of Basic Energy Sciences, of the U.S. Department of Energy under Contract No. DE-AC02-05CH11231. The TNKS1/35 data collection was performed on the X06SA beamline at the Swiss Light Source, Paul Scherrer Institut, Villigen, Switzerland.

ABBREVIATIONS USED

PARP, poly(ADP-ribose) polymerase; LipE, lipophilic efficiency; MMP, molecular matched pair; SAR, structure−activity relationship; SER, structure−efficiency relationship

REFERENCES

(1) Schreiber, V.; Dantzer, F.; Ame, J. C.; de Murcia, G. Poly(ADP-ribose): nNovel functions for an old molecule. *Nat. Rev. Mol. Cell Biol.* **2006**, *7*, 517−528.

(2) Hsiao, S. J.; Smith, S. Tankyrase function at telomeres, spindle poles, and beyond. *Biochimie* **2008**, *90*, 83−92.

(3) Seimiya, H. The telomeric PARP, tankyrases, as targets for cancer therapy. *Br. J. Cancer* **2006**, *94*, 341−345.

(4) Levaot, N.; Voytyuk, O.; Dimitriou, I.; Sircoulomb, F.; Chandrakumar, A.; Deckert, M.; Krzyzanowski, P. M.; Scotter, A.; Gu, S.; Janmohamed, S.; Cong, F.; Simoncic, P. D.; Ueki, Y.; La, R. J.; Rottapel, R. Loss of tankyrase-mediated destruction of 3BP2 is the underlying pathogenic mechanism of cherubism. *Cell* **2011**, *147*, 1324−1339.

(5) Huang, S. M.; Mishina, Y. M.; Liu, S.; Cheung, A.; Stegmeier, F.; Michaud, G. A.; Charlat, O.; Wiellette, E.; Zhang, Y.; Wiessner, S.; Hild, M.; Shi, X.; Wilson, C. J.; Mickanin, C.; Myer, V.; Fazal, A.; Tomlinson, R.; Serluca, F.; Shao, W.; Cheng, H.; Shultz, M.; Rau, C.; Schirle, M.; Schlegl, J.; Ghidelli, S.; Fawell, S.; Lu, C.; Curtis, D.; Kirschner, M. W.; Lengauer, C.; Finan, P. M.; Tallarico, J. A.; Bouwmeester, T.; Porter, J. A.; Bauer, A.; Cong, F. Tankyrase inhibition stabilizes axin and antagonizes Wnt signalling. *Nature* **2009**, *461*, 614−620.

(6) Guettler, S.; LaRose, J.; Petsalaki, E.; Gish, G.; Scotter, A.; Pawson, T.; Rottapel, R.; Sicheri, F. Structural basis and sequence rules for substrate recognition by tankyrase explain the basis for cherubism disease. *Cell* **2011**, *147*, 1340−1354.

(7) Cheung, A. K.; Chin, D. N.; Fan, J.; Shultz, M. D.; Tomlinson, R. C. 4-Oxo-3,5,7,8-Tetrahydro-4h-Pyrano {4,3-D} Pyrminidinyl Compounds For Use As Tankyrase Inhibitors. WO 2013010092, US 2011-507313P, 2013.

(8) Gunaydin, H.; Gu, Y.; Huang, X. Novel binding mode of a potent and selective tankyrase inhibitor. *PLoS One* **2012**, *7*, e33740.

(9) Shultz, M. D.; Kirby, C. A.; Stams, T.; Chin, D. N.; Blank, J.; Charlat, O.; Cheng, H.; Cheung, A.; Cong, F.; Feng, Y.; Fortin, P. D.; Hood, T.; Tyagi, V.; Xu, M.; Zhang, B.; Shao, W. [1,2,4]Triazol-3-ylsulfanylmethyl)-3-phenyl-[1,2,4]oxadiazoles: Antagonists of the Wnt pathway that inhibit tankyrases 1 and 2 via novel adenosine pocket binding. *J. Med. Chem.* **2012**, *55*, 1127−1136.

(10) Waaler, J.; Machon, O.; Tumova, L.; Dinh, H.; Korinek, V.; Wilson, S. R.; Paulsen, J. E.; Pedersen, N. M.; Eide, T. J.; Machonova, O.; Gradl, D.; Voronkov, A.; von Kries, J. P.; Krauss, S. A novel tankyrase inhibitor decreases canonical Wnt signaling in colon carcinoma cells and reduces tumor growth in conditional APC mutant mice. *Cancer Res.* **2012**, *72*, 2822−2832.

(11) Distler, A.; Deloch, L.; Huang, J.; Dees, C.; Lin, N. Y.; Palumbo-Zerr, K.; Beyer, C.; Weidemann, A.; Distler, O.; Schett, G.; Distler, J. H. Inactivation of tankyrases reduces experimental fibrosis by inhibiting canonical Wnt signalling*Ann. Rheum. Dis.* **2012**, doi: 10.1136/annrheumdis-2012-202275.

(12) Li, Z.; Yamauchi, Y.; Kamakura, M.; Murayama, T.; Goshima, F.; Kimura, H.; Nishiyama, Y. Herpes simplex virus requires poly(ADP-ribose) polymerase activity for efficient replication and induces extracellular signal-related kinase-dependent phosphorylation and ICP0-dependent nuclear localization of tankyrase 1. *J. Virol.* **2012**, *86*, 492−503.

(13) Tenbaum, S. P.; Ordonez-Moran, P.; Puig, I.; Chicote, I.; Arques, O.; Landolfi, S.; Fernandez, Y.; Herance, J. R.; Gispert, J. D.; Mendizabal, L.; Aguilar, S.; Cajal, S.; Schwartz, S., Jr.; Vivancos, A.; Espin, E.; Rojas, S.; Baselga, J.; Tabernero, J.; Munoz, A.; Palmer, H. G. Beta-catenin confers resistance to PI3K and AKT inhibitors and subverts FOXO3a to promote metastasis in colon cancer. *Nat. Med.* **2012**, *18*, 892−901.

(14) Ulsamer, A.; Wei, Y.; Kim, K. K.; Tan, K.; Wheeler, S.; Xi, Y.; Thies, R. S.; Chapman, H. A. Axin pathway activity regulates in vivo pY654-beta-catenin accumulation and pulmonary fibrosis. *J. Biol. Chem.* **2012**, *287*, 5164−5172.

(15) Fancy, S. P. J.; Harrington, E. P.; Yuen, T. J.; Silbereis, J. C.; Zhao, C.; Baranzini, S. E.; Bruce, C. C.; Otero, J. J.; Huang, E. J.; Nusse, R.; Franklin, R. J. M.; Rowitch, D. H. Axin2 as regulatory and therapeutic target in newborn brain injury and remyelination. *Nat. Neurosci.* **2011**, *14*, 1009−1U99.

(16) Bregman, H.; Gunaydin, H.; Gu, Y.; Schneider, S.; Wilson, C.; DiMauro, E. F.; Huang, X. Discovery of a class of novel tankyrase inhibitors that bind to both the nicotinamide pocket and the induced pocket. *J. Med. Chem.* **2013**, *56*, 1341−1345.

(17) Lau, T.; Chan, E.; Callow, M.; Waaler, J.; Boggs, J.; Blake, R. A.; Magnuson, S.; Sambrone, A.; Schutten, M.; Firestein, R.; Machon, O.; Korinek, V.; Choo, E.; Diaz, D.; Merchant, M.; Polakis, P.; Holsworth, D. D.; Krauss, S.; Costa, M. A novel tankyrase small-molecule inhibitor suppresses APC mutation-driven colorectal tumor growth. *Cancer Res.* **2013**, *73*, 3132−3144.

(18) Voronkov, A.; Holsworth, D. D.; Waaler, J.; Wilson, S. R.; Ekblad, B.; Perdreau-Dahl, H.; Dinh, H.; Drewes, G.; Hopf, C.; Morth, J. P.; Krauss, S. Structural basis and SAR for G007-LK, a lead stage 1,2,4-triazole based specific tankyrase 1/2 inhibitor. *J. Med. Chem.* **2013**, *56*, 3012−3023.

(19) Leeson, P. D.; Springthorpe, B. The influence of drug-like concepts on decision-making in medicinal chemistry. *Nat. Rev. Drug Discovery* **2007**, *6*, 881−890.

(20) Hopkins, A. L.; Groom, C. R.; Alex, A. Ligand efficiency: a useful metric for lead selection. *Drug Discovery Today* **2004**, *9*, 430−431.
(21) Arnott, J. A.; Planey, S. L. The influence of lipophilicity in drug discovery and design. *Expert Opin. Drug Discovery* **2012**, *7*, 863−875.
(22) Griffen, E.; Leach, A. G.; Robb, G. R.; Warner, D. J. Matched molecular pairs as a medicinal chemistry tool. *J. Med. Chem.* **2011**, *54*, 7739−7750.
(23) Trunzer, M.; Faller, B.; Zimmerlin, A. Metabolic soft spot identification and compound optimization in early discovery phases using MetaSite and LC-MS/MS validation. *J. Med. Chem.* **2009**, *52*, 329−335.
(24) Cruciani, G.; Carosati, E.; De, B. B.; Ethirajulu, K.; Mackie, C.; Howe, T.; Vianello, R. MetaSite: understanding metabolism in human cytochromes from the perspective of the chemist. *J. Med. Chem.* **2005**, *48*, 6970−6979.
(25) T'jollyn, H.; Boussery, K.; Mortishire-Smith, R. J.; Coe, K.; De, B. B.; Van Bocxlaer, J. F.; Mannens, G. Evaluation of three state-of-the-art metabolite prediction software packages (Meteor, MetaSite, and StarDrop) through independent and synergistic use. *Drug Metab. Dispos.* **2011**, *39*, 2066−2075.
(26) Shin, Y. G.; Le, H.; Khojasteh, C.; Hop, C. E. Comparison of metabolic soft spot predictions of CYP3A4, CYP2C9 and CYP2D6 substrates using MetaSite and StarDrop. *Comb. Chem. High Throughput Screening* **2011**, *14*, 811−823.
(27) Storni, A. *Carboxamides*. EP 124476, Nov 7, 1984.
(28) Bregman, H.; Chakka, N.; Guzman-Perez, A.; Gunaydin, H.; Gu, Y.; Huang, X.; Berry, V.; Liu, J.; Teffera, Y.; Huang, L.; Egge, B.; Mullady, E. L.; Schneider, S.; Andrews, P. S.; Mishra, A.; Newcomb, J.; Serafino, R.; Strathdee, C. A.; Turci, S. M.; Wilson, C.; DiMauro, E. F. Discovery of novel, induced-pocket binding oxazolidinones as potent, selective, and orally bioavailable tankyrase inhibitors. *J. Med. Chem.* **2013**, *56*, 4320−4342.
(29) Tsukamoto, A. S.; Grosschedl, R.; Guzman, R. C.; Parslow, T.; Varmus, H. E. Expression of the int-1 gene in transgenic mice is associated with mammary gland hyperplasia and adenocarcinomas in male and female mice. *Cell* **1988**, *55*, 619−625.
(30) Freire, E. Do enthalpy and entropy distinguish first in class from best in class? *Drug Discovery Today* **2008**, *13*, 869−874.
(31) Conroy, J. L.; Sanders, T. C.; Seto, C. T. Using the electrostatic field effect to design a new class of inhibitors for cysteine proteases. *J. Am. Chem. Soc.* **1997**, *119*, 4285−4291.
(32) Karlberg, T.; Markova, N.; Johansson, I.; Hammarstrom, M.; Schutz, P.; Weigelt, J.; Schuler, H. Structural basis for the interaction between tankyrase-2 and a potent Wnt-signaling inhibitor. *J. Med. Chem.* **2010**, *53*, 5352−5355.